# Multidimensional perovskites : a mixed cation approach towards ambient stable and tunable perovskite photovoltaics

Koh, Teck Ming; Thirumal, Krishnamoorthy; Soo, Han Sen; Mathews, Nripan

2016

Koh, T. M., Thirumal, K., Soo, H. S., & Mathews, N. (2016). Multidimensional perovskites : a mixed cation approach towards ambient stable and tunable perovskite photovoltaics. ChemSusChem, 9(18), 2541-2558. doi:10.1002/cssc.201601025

https://hdl.handle.net/10356/142099

https://doi.org/10.1002/cssc.201601025

# Multidimensional Perovskites: A Mixed Cation Approach Towards Ambient Stable and Tunable Perovskite Photovoltaics

Dr. Teck Ming Koh, Krishnamoorthy Thirumal, Prof. Han Sen Soo, Prof. Nripan Mathews

Although halide perovskites are able to deliver high power conversion efficiencies, their ambient stability still remains an obstacle for commercialization. Thus, promoting the ambient stability of perovskites has become a key research focus. In this review, we highlight the sources of instability in conventional 3 D perovskites, including water intercalation, ion migration, and thermal decomposition. Recently, the multidimensional perovskites approach has become one of the most promising strategies to enhance the stability of perovskites. As compared to pure 2 D perovskites, multidimensional perovskites typically possess more ideal band gaps, better charge transport, and lower exciton binding energy, which are essential for photovoltaic applications. The larger organic cations in multidimensional perovskites could also be more chemically stable at higher temperatures than the commonly used methylammonium cation. By combining 3 D and 2 D perovskites to form multidimensional perovskites, halide perovskite photovoltaics can attain both high efficiency and increased stability.

## 1 Introduction

The impending crisis of global climate change and the anticipated damage to the global economy and natural environment has brought renewed focus on the inexorable rise of atmospheric $CO_2$ levels.[1] One of the most sustainable and technologically feasible solutions is to harvest solar energy with photovoltaics (PVs) for electricity generation.[2] With a wide variety of photovoltaic technologies available, solar cells that could be facilely formed from low-energy intensive processes are in focus. In this context, perovskite solar cells (PSCs), which can be easily solution processed, have emerged as the leading contender for future low-cost electricity production.[3]

When organic–inorganic metal halide perovskites were first incorporated as photosensitizers into sensitized solar cells in 2009, the power conversion efficiency (PCE) was a modest, but notable value of 3.8 %.[4] In the mere seven years since then, solid-state PSCs in various architectures, including the meso-superstructured scaffold,[5] the planar structure,[6] and even metal oxide-free geometries,[7] have been developed with PCEs ranging from 18 to over 22 %[8] Proof of concept tandem perovskite–Si solar cells have achieved outstanding PCEs of up to 25.2 %.[9] PSCs, comprised entirely of Earth-abundant elements, can be manufactured in various geometries, solutionprocessed, and have optical band gaps ($E_g$) of around 1.5 eV; producing PVs with such PCE values that they can be now considered as solution processable forms of solar cell workhorses, such as Si or GaAs.[8, 10]This meteoric rise in PCEs has created a renaissance in studies on (organic–inorganic) metal halide perovskites for light-emitting diodes,[11] lasing,[12] photodetectors,[13] field-effect transistors,[14] and non-linear optical materials,[15] among others.

However, PSCs that have been developed are also notoriously unstable, especially over the long-term under ambient, atmospheric conditions.[8, 10] A deeper understanding of the instability and cost-effective solutions to circumvent them will be vital for the eventual deployment of PSCs to consumers worldwide. We present an analysis of the recognized origins of instability among the perovskites deployed for PSCs.[10, 16] We offer some approaches to surmount the vexing

instability issues that will be detrimental to PSCs through inherent materials science solutions by the utilization of multidimensional perovskites.[17]

## 2 Sources of Instability in Conventional 3 D Perovskites

Despite the large number of primary studies documenting the suspect stability of PSCs under various operating and model conditions, there has been a dearth of reports that summarize the cumulative insights. A recent review included some of the progress in improving the chemical stability of PSCs, but omitted discussions on lead-free perovskites and ionic migration within PSCs.[18] We present herein a systematic evaluation of the reasons for instability in methylammonium lead halide ($MAPbX_3$) and formamidinium lead halide ($FAPbX_3$) perovskites, and follow up with promising strategies to overcome the problems with multidimensional perovskites.

### 2.1 Moisture complexation

The effect of water on PSCs has received considerable attention owing to the ubiquitous presence of water (from rain) and humidity (from water vapor in air) in all realistic operating conditions of solar cells when exposed to the weathering elements. We will distinguish the roles of water during the fabrication process from the presence of water under operating conditions. While water has been shown to be beneficial for the fabrication of PSCs under precisely controlled situations,[6, 19] exposure to even humid environments has invariably led to compromised performance for the PSCs, with the severity depending on the length of exposure and amount of water.[10, 18, 20]

Water, being a base and ligand, had initially been thought to be detrimental for the production of PSCs. However, Zhou et al. reported that perovskite films grown in air with controlled 30 % relative humidity (RH) surprisingly displayed increased photoluminescence (PL) lifetimes, open-circuit potentials ($V_{OC}$), and fill factors (FF).[6] Likewise, another report suggested moisture enhancement on film formation of $MAPbI_3$ and $MAPbBr_3$ when the films were cast in air at 58.2 % RH, in comparison to films deposited in an Ar-filled glovebox.[19a] The moisture was found to trigger crystallization and the films that formed with humidity showed two orders of magnitude higher PL lifetimes for $MAPbBr_3$.[19a] Snaith and coworkers have found that by steadily increasing the RH, an optimal RH level of 50 % provided PCEs of above 14 %.[19b] A mechanism where water facilitates the removal of excess $MA^+$, hence filling in trap states and minimizing non-radiative recombinations, was proposed.[19b] Nonetheless, extended annealing at 30 % RH led to gradual film degradation.[19b] The damage to $MAPbI_3$ by water vapor appears to be reversible, provided that the perovskite has not come into contact with liquid water (vide infra).[10, 21] Docampo, Barnes, and coworkers exposed $MAPbI_3$ single crystals, polycrystalline materials, and thin films to air at 80 % RH and confirmed that a monohydrate formed [Eq. (1)], but could be reversed by blowing dry air over the material.[21] These results concur with several prior investigations, which indicate that other Lewis-basic small-molecule solvents, such as acetone, acetonitrile, nitromethane, isopropanol, *N* ,*N* -dimethylformamide, and dimethylsulfoxide, are all capable of reversibly infiltrating the perovskite lattice, both during and postfabrication.[20b, 20d, 22] The small Lewis bases insert readily through hydrogen-bonding interactions to disrupt the 3 D perovskite structure. Nevertheless, the non-covalent interactions appear to be weak and the volatile small molecules can be ejected by heat, vacuum, or even mere treatment with dry gases.

$$(CH_3NH_3)PbI_3 + H_2O \rightleftharpoons (CH_3NH_3)PbI_3 \cdot H_2O \quad (1)$$

Despite the early recognition of the detrimental impact of water on PSCs, the mechanism for irreversible degradation was not established until recently. Some preliminary speculative perovskite degradation pathways included the deprotonation of methylammonium by catalytic amounts of the weakly basic water to release volatile $CH_3NH_2$ and HI.[18, 23] However, this decomposition route has never been experimentally verified and is inconsistent with the significantly higher pKa of $CH_3NH_3^+$ compared to $H_3O^+$. Instead, several groups have converged on an alternative proposal, which concurs with the porous nature of the $MAPbI_3$ structure. Yang et al. employed in situ optical absorption spectroscopy and grazing incidence X-ray diffraction to identify an intermediate phase that was neither $MAPbI_3$ nor $PbI_2$, but was the hydrated molecule $MA_4PbI_6{\cdot}2\,H_2O$.[20d, 20e] Docampo, Barnes, and coworkers had utilized powder X-ray diffraction (pXRD), and single-crystal XRD studies to unequivocally establish that $MA_4PbI_6{\cdot}2\,H_2O$ formed through the intermediacy of $MAPbI_3{\cdot}H_2O$ (Figure 1).[21] Excess water shifted the equilibrium towards conversion of $MAPbI_3{\cdot}H_2O$ to $MA_4PbI_6{\cdot}2\,H_2O$ and $PbI_2$ [Eq. (2)], before phase separation led to the eventual irreversible dissolution and loss of MAI [Eq. (3)].[21] Other mechanisms may be concurrently operational and could be uncovered, but these water-intercalation and solubilization processes are the most plausible and empirically supported routes for rationalizing the instability of PSCs after exposure to humid environments.

$$4\,[(CH_3NH_3)PbI_3 \cdot H_2O] \rightleftharpoons (CH_3NH_3)_4PbI_6 \cdot 2\,H_2O + 3\,PbI_2 + 2\,H_2O \quad (2)$$

$$(CH_3NH_3)_4PbI_6 \cdot 2\,H_2O \rightarrow 4\,CH_3NH_3I + PbI_2 + 2\,H_2O \quad (3)$$

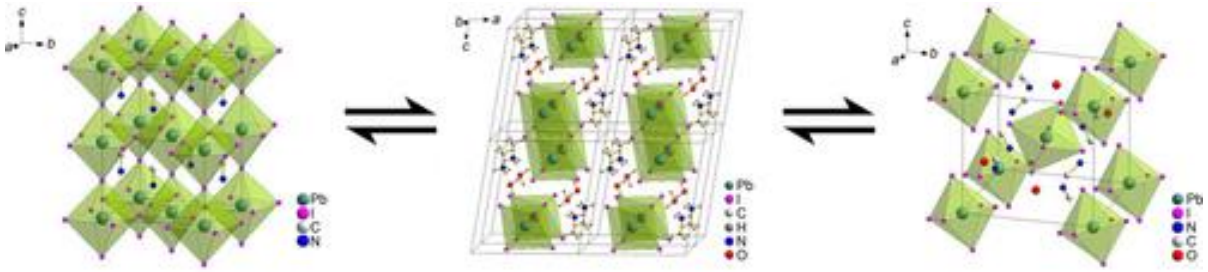


**Figure 1.** Reproduced crystal structure changes from cubic $MAPbI_3$ to $MAPbI_3{\cdot}H_2O$, before converting to the dihydrate $MA_4PbI_6{\cdot}2\,H_2O$. Adapted from Ref. **21**. Copyright 2015 American Chemical Society.

## 2.2 Ion migration

The low enthalpies of formation of the perovskites from their components facilitate the interchange of ionic species and realization of several new materials in a short span of time. The benefits of mixed cation systems for truly impressive PCEs, even including a combination of $MA^+$, $FA^+$, and $Cs^+$, have been demonstrated, although most of the cations were mixed during fabrication.**24** Halide exchange has been adopted to create mixed halide perovskites with tunable PL wavelengths that cover the entire visible spectrum.**25** The rapid ionexchange reactions allude to facile ion migration in PSCs, but the identity and circumstances for ion conduction has remained uncertain because of the reversible processes and the lack of spatial distribution of the elemental composition in operando. Gratifyingly, a series of theoretical and experimental investigations have

unequivocally established that halide, ammonium, and perhaps even proton migration occur to (transiently) deteriorate the perovskite optoelectronic properties.

Earlier studies on lead halides and inorganic perovskites had shown that anion migration through vacancy sites had low activation energies below 0.4 eV, which would be thermally accessible at 298 K.[26] The observation of photocurrent–voltage hysteresis among PSCs prompted a thorough analysis to explore if the bias asymmetry arose from intrinsic material properties or processing deficiencies. Among the popular explanations that included ferroelectricity and ion migration, the latter has emerged as the likelier reason for the unusual hysteresis phenomena even in high-quality perovskite films.[16a, 26b] Although all the component ions of $MAPbI_3$ including $Pb^{2+}$, $MA^+$, $H^+$, and $I^-$ could possibly conduct, realistically, vacancies, and short migrating distances dictate the feasibility of the ion migration. Interstitial hydrogen impurities are expected to migrate as $H^+$ with low activation energies ($E_a$) of less than 0.30 eV, by distorting the neighboring $I^-$ lattice through hydrogen bonding.[27] A number of papers involving density functional theory (DFT) calculations with different levels of sophistication appeared almost concurrently to predict the $E_a$ of $MAPbI_3$ (and also $MAPbBr_3$ and $FAPbI_3$).[28] Fortunately, all of them forecast the same trends in activation energy: $I^-<MA^+<FA^+<Pb^{2+}$, albeit with a wide distribution in absolute energies.[28a–28c] The $E_a$ for $I^-$ migration ranged from 0.08–0.58 eV, while the $E_a$ for $MA^+$ migration was expected to be between 0.46–0.89 eV.[28a–28c] The monoanionic $I^-$ ions have the shortest predicted path for migration between adjacent edges sites (Figure 2 a), whereas both the $MA^+$ and $Pb^{2+}$ cations have to traverse at least a unit-cell length to fill up vacancies (Figure 2 b and 2 c).[28a]

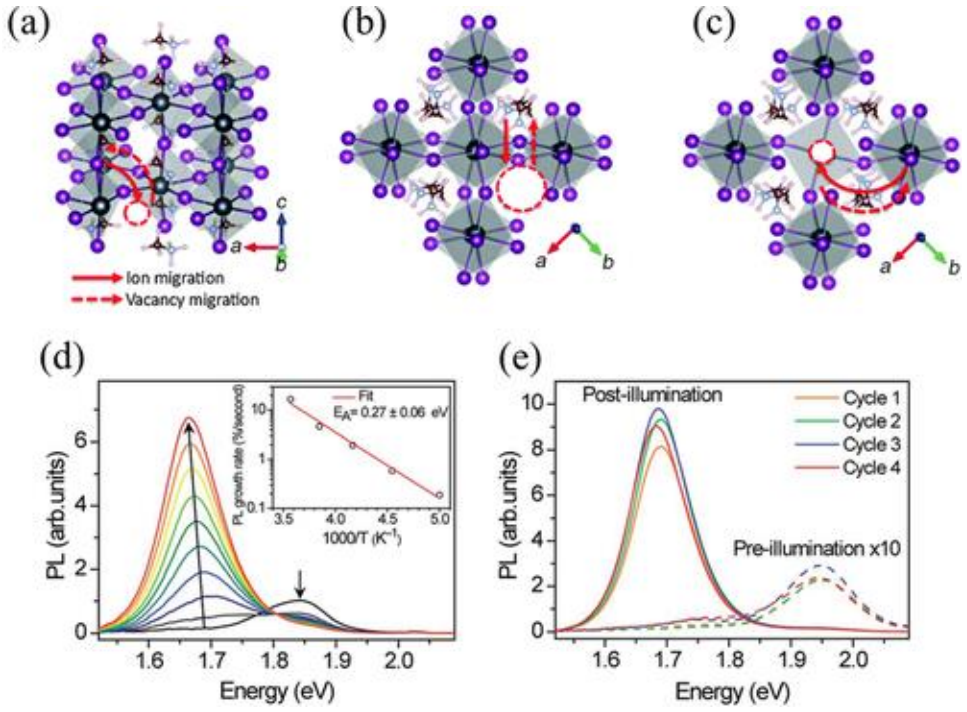


**Figure 2**. Ion and vacancy migration paths predicted by DFT calculations for (a) $I^-$, (b) $MA^+$, and (c) $Pb^{2+}$. The red broken circles represent vacancies, the solid lines indicate ion trajectory, and the dashed lines indicate vacancy diffusion. The color code for atoms is as follows: Pb=black, I=purple, N=blue, C=brown, H=white. Adapted from Ref. [28a] with permission from The Royal Society of Chemistry. (d) PL spectra of an $x$ =0.4 thin film over 45 s in 5 s increments under 457

nm, 15 mW cm$^{-2}$ light at 300 K. Inset: temperature dependence of initial PL growth rate. (e) PL spectra of an $x$ =0.6 thin film after sequential cycles of illumination for 2 min (457 nm, 15 mW cm$^{-2}$ followed by 5 min in the dark). Adapted from Ref. **29** with permission from The Royal Society of Chemistry.

Hoke et al. reported the ionic motion that lead to the phase separation of $(CH_3NH_3)Pb(Br_xI_{1-x})_3$ perovskite within 1 min under 1 sun illumination.**29** These mixed-halide perovskites showed an additional PL peak at 1.68 eV with increasing intensity under constant illumination (Figure **2** d). The peak position of this new peak is independent of halide composition and $E_g$. This phenomenon is reversible and the original PL signal is recovered after turning off the light for 5 min (Figure **2** e). The new PL signature of the mixed halide perovskites is a result of the formation small I$^-$-rich domains with a smaller $E_g$ compared to homogenously mixed perovskites. Overall, there is now explicit evidence that I$^-$ and MA$^+$ can migrate under idealized electrostatic or radiative impetus, with detrimental consequences on the optoelectronic properties. However, the ionic migration may not be permanent, and future studies of high quality, reproducible PSCs in operando will be necessary to decide if ion migration will pose intractable instability issues.
Crucially, I$^-$ migration leading to interfacial degradation and phase segregation appeared to be a prevalent problem for PSCs under both applied electric fields and photodriven conditions. Yang et al. created a solid-state electrochemical cell consisting of Pb|$MAPbI_3$|AgI|Ag (Figure 3 a) to monitor ionic movement. Such a coulometric cell configuration with one electronic (Pb) and one ionic electrode (AgI|Ag) causes chemical changes during current flow. The investigation of chemical effects at the various interfaces upon long-term charge transference (the Pb electrode taken as plus and the Ag electrode as minus pole) allows for the identification of the moving ions.30 Energy dispersive X-ray spectroscopy (EDX) and pXRD experiments unambiguously validated corrosion of the Pb anode partially to $PbI_2$, while the cathode showed no notable alterations.30 In another study, deQuilettes et al. utilized confocal fluorescence imaging to illustrate that the PL intensity generally increased throughout the film during light soaking, but reduced to different levels at disparate locations after the illumination ceased (Figure 3 b).31 Depth profiling by time of flight-secondary ion mass spectrometry indicated that the locations with highest irradiation intensity displayed diminished levels of I$^-$ ions, whereas the surrounding regions had elevated I$^-$ concentrations.31 Electrical poling at slightly elevated temperatures of 330 K applied to a $MAPbI_3$ film exhibited a "$PbI_2$ thread" by optical microscopy (Figure 3 c).32 The authors propose both I$^-$ and MA$^+$ migration in opposite directions as the origin of this interesting observation.32 At 330 K, $MAPbI_3$ is more labile and can decompose to $PbI_2$ as shown in Equation (4). When a potential was first applied at the anode, some of the I$^-$ would be oxidized to $I_2$ [Eq. (5)], leading to the formation of the $PbI_2$ thread.32 The applied potential would draw more I$^-$ anions toward the anode (left to right in Figure 3 c), whereas the MA$^+$ cations are drawn to the cathode (right to left). Consequently, the right interface is where $MAPbI_3$ while the left interface is where the perovskite breaks down, thus creating this illusion of a traversing $PbI_2$ thread.32

$$(CH_3NH_3)PbI_3 \rightleftharpoons PbI_2 + CH_3NH_3^+ + I^- \quad (4)$$

$$2I^- \rightarrow I_2\ (g) + 2e^- \quad (5)$$

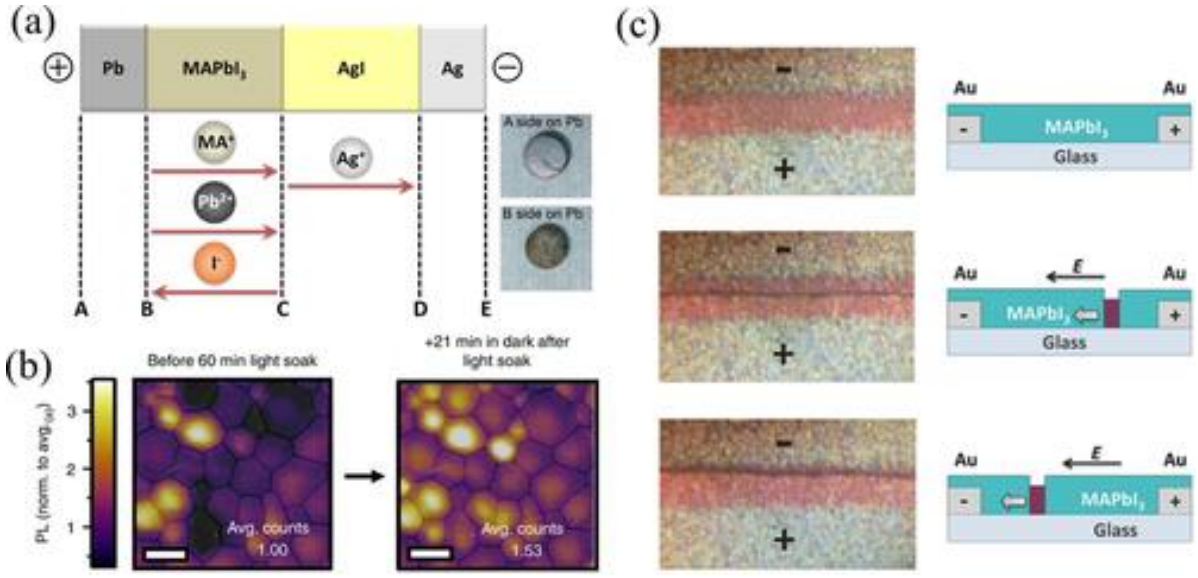


**Figure 3**. (a) Flow directions of the charged ion species in a Pb|$MAPbI_3$|AgI|Ag cell under electrical bias. Inset photographs show the images for surfaces A and B. Reproduced from Ref. **30** with permission from Wiley-VCH Verlag GmbH & Co. KGaA. (b) Confocal fluorescence imaging with pulsed 470 nm excitation measured by SEM showing the PL before illumination and 21 min after light soaking. The scale bar shows 1 μm. Adapted from Ref. **31** with permission from the Nature Publishing Group. (c) Trajectory of the $PbI_2$ thread (grey horizontal band) from the cathode to the anode on the left with a cartoon depiction of the process on the right. Adapted from Ref. **32** with permission from Wiley-VCH Verlag GmbH & Co. KGaA.

Likewise, Yuan et al. applied similar electrical poling under ambient temperatures on a $MAPbI_3$ film and employed photothermal-induced resonance microscopy to detect movement of $MA^+$ ions from the anode to the cathode under constant potential.**33**

2.3 Thermal instabilities

In general, prolonged exposure to high temperatures would damage the perovskite structure through thermal degradation. Furthermore, some of the perovskite crystal structures are temperature dependent, whereby the crystal structures may alter at different temperatures. These temperature-induced changes could potentially reduce the perovskite's light-harvesting capability ($E_g$ variation) or alter charge transport (owing to structural transitions), and ultimately affect the PV performances. Here, we considered two types of thermal instabilities, namely the effects of thermally induced chemical decomposition and phase transition in perovskites.

A number of theoretical and experimental studies have concluded that $MAPbI_3$ exhibits very low heat conductivity,**16c**, **34** which may be a contributing factor for poor thermal dissipation and hence mechanical stress in PSCs.**18** Wang and Lin recently discussed the use of equilibrium molecular dynamics (MD) on the orthorhombic, tetragonal, and cubic phases of $MAPbI_3$ to demonstrate that remarkably low phonon thermal transport exists, arising from short phonon lifetimes and mean free paths, as well as low elastic stiffness.**16c** At room temperature and typical operating temperatures, $MAPbI_3$ remains in the tetragonal phase, which possesses thermal conductivity ($\kappa$) of around 0.31 W $m^{-1}$ $K^{-1}$ (Figure **4** a).**16c** Although high frequency vibrational modes exist in $MAPbI_3$ (1000–3350 $cm^{-1}$), most of them can be attributed to localized stretching and bending modes in $MA^+$, which are uncoupled, have low group velocities, and do not distribute

heat.[16c] Interestingly, the authors pointed out that the lighter elements Sn for Pb and Br for I should have higher thermal conductivities by virtue of the stronger M–X ionic interactions, higher Young's modulus, and likewise higher group phonon velocities.[16c] Pisoni et al. had carried out thermal conductivity measurements on single crystalline and polycrystalline samples that mirrored the theoretical predictions qualitatively (Figure 4 b), lending credence to the remarkably low heat-transfer model of $MAPbI_3$ developed thus far.[34b]

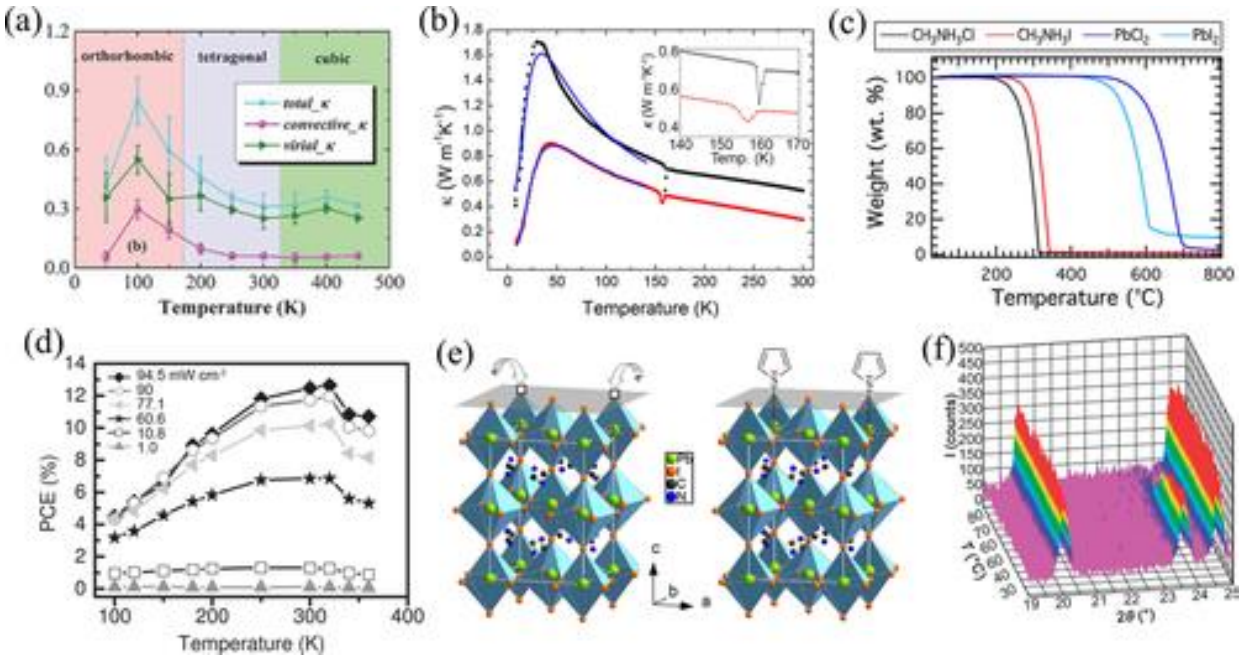


**Figure 4**. (a) The components of the thermal conductivity ($\kappa$) and their variation with temperature across the three stable phases in the labelled regions, predicted by equilibrium molecular dynamics. Adapted from Ref. [16c] with permission from Wiley-VCH Verlag GmbH & Co. KGaA. (b) Experimental thermal conductivity dependence on temperature for single crystal (black) and polycrystalline (red) $MAPbI_3$ samples. The blue lines are modeled while the inset illustrates an expansion of the structural transition at 160 K. Adapted from Ref. [34b]. Copyright 2014 American Chemical Society. (c) TGA heating curves of individual precursor powders expressed in wt % as a function of applied temperatures and the corresponding first derivatives. Adapted from Ref. [35]. Copyright 2014 American Chemical Society. (d) Temperature dependence of PCE measured for different irradiance values. Adapted from Ref. [36] with permission from Wiley-VCH Verlag GmbH & Co. KGaA. (e) Undercoordinated Pb sites creating $I^-$ vacancies and hence a net positive charge on the green Pb atoms ($\delta+$). These will become Coulomb traps for photogenerated electrons. The electron traps can be passivated with thiophene (or pyridine) by formation of a coordinate bond. Adapted from Ref. [37]. Copyright 2014 American Chemical Society. (f) 3 D plot of the pXRD patterns as functions of temperature, which show the gradual disappearance of the {2 1 1} reflection associated with the tetragonal supercell. Adapted from Ref. [39] with permission from The Royal Society of Chemistry 2013.

### 2.3.1 Thermally induced chemical decomposition

Organic cations (such as $MA^+$ and $FA^+$) are labile with low enthalpies of formation and can be easily liberated at high temperatures. In a recent study, Dualeh et al. examined the thermal

properties of the $MAPbX_3$ (X=I or Cl) perovskites using thermogravimetric analysis (TGA, Figure 4 c).[35] The organic component of the perovskite decomposes by the loss of HI and $CH_3NH_2$, which will be detrimental to the long-term stability of PSCs (Figure 4 d).[36] During the thermal annealing process, $MA^+$ and $I^-$ could be lost at the crystal interface with charge-transporting layers, leading to under-coordinated Pb sites.[37] By introducing Lewis bases, such as pyridine and thiophene, the iodide vacancies could be passivated so that they were no longer Coulomb traps for electrons (Figure 4 e).[37] The authors observed an order-of-magnitude increase in PL lifetime, translating to an increase in the charge-diffusion length to about 3 μm.[37] Using a similar strategy, iodopentafluorobenzene (IPFB) was used to cap the under-coordinated terminal $I^-$ sites through exploitation of halogen bonding between the partial positive charge on the IPFB iodine and the electron-rich terminal $I^-$ at the interface with charge-transport layers.[38] It was suggested that the IPFB prevented the terminal, under-coordinated $I^-$ from acting as hole traps, which resulted in an increase in the PCE from 13.0 to >15 %,[38] thus emphasizing the potential tactic of appropriate interfacial engineering for improved PSC performance.

### 2.3.2 Phase transitions

The phase-transition temperature of $MAPbI_3$ from tetragonal to cubic structure was determined to be at approximately 57 °C (Figure 4 f), which could potentially affect its PV performance owing to the altered conductivity at temperatures higher than the phase-transition temperature.[39] Moreover volume changes associated with the phase transition could result in long-term delamination. In view of the thermal instability associated with $MA^+$, replacement of $MA^+$ with other cations is required. An alternative to the $MA^+$ cation in the organic–inorganic metal halide perovskites is the $FA^+$ cation $[HC(NH_2)_2^+]$, which was first introduced as a mixture with $MA^+$ into PSCs in 2014.[5, 9, 24b, 40] $FAPbI_3$ is more stable at room temperature as the non-perovskite yellow, hexagonal ($P\,6mc$) $\delta$-phase, which consists of 1 D arrays of $PbI_6$ octahedra.[41] The black perovskite, trigonal ($P\,3m\,1$) phase was accessed by heating above 333 K and has the ideal $E_g$ of 1.48 eV, smaller than the $E_g$ of around 1.55 eV for $MAPbI_3$.[41] Owing to the attractive hole-diffusion length (~813 nm), electron diffusion length (~177 nm), appropriate $E_g$, and greater thermal stability relative to $MAPbI_3$, the complicated phase diagram of $FAPbI_3$ has not deterred efforts on improved fabrication techniques for incorporation into PSCs.[24b, 42] In fact, $FA^+$ has now emerged as the preferred organic cation in mixed organic–inorganic cationic combinations for some of the best PSCs to date.[5, 9, 24b]

Unfortunately, other 3 D analogues have unsuitable $E_g$ at solar cell operating temperatures. $CsPbI_3$ exists at room temperature in the yellow orthorhombic phase, which may convert to the more desirable black perovskite phase only at around 305 °C.[43] Although the other halides $CsPbCl_3$ and $CsPbBr_3$ retain the perovskite phase under ambient conditions, the former is pale yellow while the latter is orange, suggesting that their $E_g$ are too large for them to absorb the solar spectrum efficiently.[43] The mixed metal iodides ($AMI_3$, A=Rb or Cs, M=Pb) were revisited more recently and the yellow $CsPbI_3$ was confirmed with the orthorhombic *Pnma* space group at 298 K,

while the black cubic *Pm m* structure formed between 563–602 K (290–329 °C).[44] The $RbPbI_3$ did not convert from the yellow *Pnma* isomorph even at temperatures up to 634 K.[44]

2.4 Other possible degradation pathways

There have been few reports demonstrating that irradiating an unencapsulated perovskite film spin-coated onto nanocrystalline $TiO_2$ resulted in PCE deterioration, while insertion of a layer (e.g., $Sb_2S_3$) resulted in retention of the PCE.[45] The authors proposed that the $TiO_2$–$MAPbI_3$ interface was the site for oxidative degradation owing to the anticipated oxidizing power of holes in $TiO_2$ generated during light soaking. On illumination over extended periods, the $TiO_2$ can absorb UV radiation to form separated holes ($h^+$) and electrons ($e^-$), of which the $h^+$ would be able to oxidize $I^-$ to $I_2$. The $e^-$ would reduce the $I_2$ formed in the presence of $MA^+$ to give the volatile gases HI and $CH_3NH_2$, thus leading to the phase separation of $PbI_2$ at the interface with $TiO_2$. With a $Sb_2S_3$ blocking layer inserted between $TiO_2$ and $MAPbI_3$, this destructive loss of volatile components under illumination could be prevented, giving longer-lived PSCs even without encapsulation. However, the possibility of photoexcitation in $Sb_2S_3$, which is a small $E_g$ semiconductor ($E_g$=1.7 eV) was not considered by the authors. Along the same lines, Snaith and coworkers had earlier reported on the instability of PSCs caused by irradiation with UV at the $TiO_2$ interface in meso-superstructured perovskite PVs.[46] Without a UV filter, the PCE and short-circuit current density ($J_{SC}$) of the encapsulated PSC plunged below 10 % of their initial values within 5 h.[46] As filtering the UV light would unrealistically compromise the PV performance, they recommended replacing the mesoporous $TiO_2$ with the insulating mesoporous $Al_2O_3$ instead to overcome these damaging processes at the $TiO_2$–$MAPbI_3$ borders.[46] On the contrary, a more recent study offered diametrically opposite guidelines on the choice of metal oxide scaffolds. When $MAPbI_3$ layers coated on mesoporous $Al_2O_3$ were irradiated with a tungsten halogen lamp under dry air for a few days, the perovskite layer decomposed to release $CH_3NH_2$ and $PbI_2$, as confirmed by pXRD, Raman spectroscopy, and EDX.[47] Superoxide $O_2^-$ (generated under illumination) acts as a base to deprotonate $MA^+$ to form $CH_3NH_2$ [Eqs. (6–8)].[47] The remaining $h^+$ would in turn oxidize $I^-$ to $I_2$, leaving $PbI_2$ behind.[47] The concentration of $O_2^-$ produced from the $MAPbI_3$ film on mesoporous $TiO_2$ sample was around three times lower than $Al_2O_3$, as efficient $e^-$ injection from the perovskite film into $TiO_2$ limited the generation of $O_2^-$.[47]

$$(CH_3NH_3)PbI_3 \rightarrow (CH_3NH_3)PbI_3^* \rightarrow (CH_3NH_3)PbI_3 + h^+ + e^- \quad (6)$$

$$e^- + O_2 \rightarrow O_2^- \quad (7)$$

$$(CH_3NH_3)PbI_3 + O_2^- \rightarrow CH_3NH_2 + PbI_2 + I^- + HOO^\bullet \quad (8)$$

### 2.4.1 Lead-free perovskites

Although PSCs containing lead halide perovskites have shown exceptional PCEs, a potentially fatal shortcoming is the toxicity of Pb and partial solubility of the Pb-based perovskites, which makes contamination from these solar cells in outdoor environments a palpable threat. In this regard, Pb-free perovskites, such as the all-inorganic $CsSnI_3$ perovskite phase, are especially appealing. However, recent studies have found, in addition to high number of defect sites in Sn-based PSCs, their propensity to oxidize from $Sn^{II}$ to $Sn^{IV}$ will hinder long-term stable operation.[48] The introduction of $SnF_2$ and $SnF_2$–pyrazine can inhibit the $Sn^{IV}$ formation.[49] Future work on more effective oxidation inhibitors, multidimensional perovskites, and enhanced interfacial engineering could eventually make high-performing Pb-free PSCs a reality.

The multiple reports highlighted above point to the deficiencies of the 3 D perovskites at different environmental conditions; however, their spectacular trajectory in PCE performance had masked these inherent instability issues with the expectation that improved engineering and encapsulation technologies could overcome the shortcomings. However, a newer generation of perovskites that would have intrinsically more stable properties would need to be developed in parallel for PSCs to be commercialized. These new perovskites should incorporate more stable organic or mixed cations, which can impart greater thermal stability and improved moisture resistance while still possessing the attractive properties of 3 D perovskites (e.g., small $E_g$, high absorption coefficients, good diffusion lengths). Multidimensional perovskites that would incorporate a wider range of organic cations with tunable properties provides a rich playground for tuning the optical, electrical, and chemical properties of the perovskite light absorber.

## 3 Multidimensional Perovskites

The archetypical perovskite is defined by the general formula $AMX_3$ (where A=Cs, $MA^+$, $FA^+$; M=$Pb^{2+}$, $Sn^{2+}$, $Ge^{2+}$, $Cu^{2+}$; X=$I^-$, $Br^-$, $Cl^-$).17a, 26b, 50 Stable perovskite structures can be formed when the ionic radii of $A^+$, $M^{2+}$, and $X^-$ are limited within the Goldschmidt tolerance [$t$, Eq. (9)] and the octahedral [$\mu$, Eq. (10)] factors defined as the following,17a, 26b, 50 respectively:

$$t = \frac{R_A + R_X}{\sqrt{2}(R_M + R_X)} \quad (9)$$

$$\mu = \frac{R_M}{R_X} \quad (10)$$

where $R_A$, $R_M$, and $R_X$ refer to the corresponding ionic radii. The majority of the stable, archetypical 3 D perovskites have values of $0.8<t<0.9$ and $0.442<\mu<0.895$, with significant deviations that result in edge-shared and face-shared octahedral, instead of the pristine corner-shared structure of the classic $AMX_3$ perovskite.**17a**, **26b**, **50**, **51** Owing to the facile synthetic procedures and versatility of the perovskite structure, a number of organic ammonium cations that do not fit within the octahedral cavities in the original 3 D perovskite structure have been prepared. Some of these adopt 2 D perovskite slabs with corner-shared octahedra, and conform to the Ruddlesden–Popper formulae $A_{n-1}A'_2M_nX_{3n+1}$, where M and X retain the same definitions, and A and A′ are typically bulkier organic ammonium cations.**52** Consequently, numerous materials with the general formulae $(RNH_3)_2(A)_{n-1}M_nX_{3n+1}$ ($n$ =integer) are now loosely called 2 D perovskites and $(RNH_3)_2(A)_mM_mX_{3m+2}$ are called 1 D perovskites, where $RNH_3$ is an aliphatic or aromatic alkylammonium cation.**53** These can be broadly classified as multidimensional perovskites (Figure **5** a), although the term 0 D perovskites are strictly just molecular crystals and will not be considered.

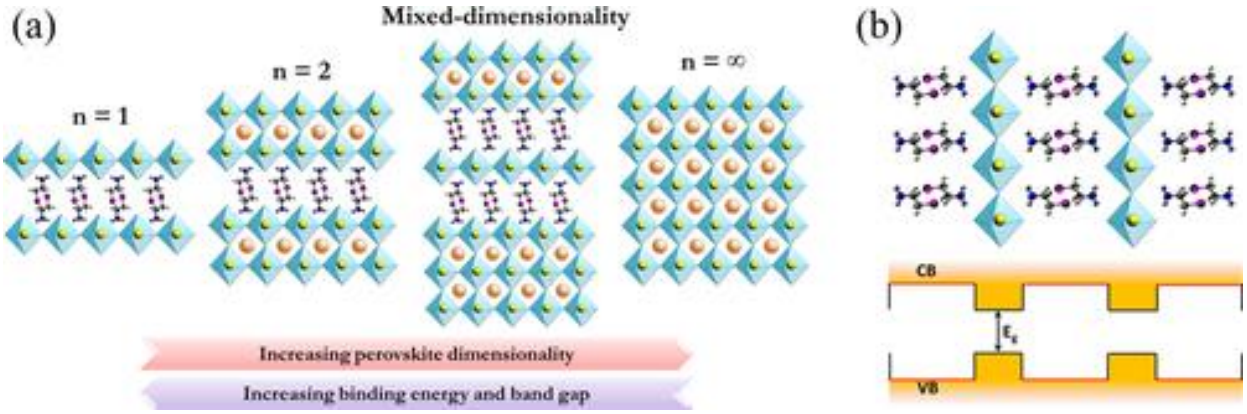


**Figure 5**. (a) Illustration showing the crystalline structure of multidimensional perovskites, including 2 D perovskites ($n$ =1 and 2, where $n$ represents the metal halide lattices), mixed-dimensional perovskites, and 3 D perovskites ($n$ =∞). Adapted from Ref. 59. Copyright 2016 Wiley-VCH Verlag GmbH & Co. KGaA. (b) Representation of the band gap ($E_g$) between the conduction and the valence band (CB and VB, respectively) in 2 D perovskites. Layered perovskites form multiple quantum wells, in which the inorganic and organic layers act as "well" and "barrier", respectively.

The ability of the corner-shared $PbX_6^{4-}$ octahedra layer to accommodate larger cations and the energy difference between the ionic bonding in the inorganic layers and the van der Waals forces among the organic molecules lead to the formation of self-assembled layered perovskites that contain alternating organic and inorganic layers.54 This unique configuration creates internal multiple quantum wells (Figure 5 b) and shows interesting photophysical properties. For instance, the HOMO–LUMO energy gap of the organic ammonium cation is typically higher than the band gap of the inorganic layers,55 and the difference in dielectric constants between these two materials create periodic barriers and wells. Hence these materials can be considered as containing a self-organized multiple quantum-well structure. The strong tendency to form layered perovskites and the solubility of both starting components in the same solvent has permitted very simple and convenient spin coating technique to deposit the thin films.56 This controlled formation of layered structures has led to perovskites with larger cations and variable structures and sizes that alter the photophysical and electronic properties of these new semiconductors.57 Adding to this versatility, mixed cations with different sizes can also form well-organized layered structures where the smaller cations occupy voids created by the corner shared $PbX_6^{4-}$ octahedral, while the larger cations cap the stacks of inorganic layers and interleave between the 2 D nanosheets.16d, 52a, 58 Some prototypical examples of mixed dimensional perovskites are $(CH_3(CH_2)_3NH_3)_2(CH_3NH_3)_2Pb_3I_{10}$ and $(CH_3(CH_2)_3NH_3)_2(CH_3NH_3)_3Pb_4I_{13}$, which crystallized as wellorganized layered structures.59 The properties, such as the $E_g$, band energy levels, carrier-binding energy, and charge transport, among others, can be easily tuned simply by varying the organic cations and the thickness of the inorganic layers.59

### 3.1 Multidimensional perovskite photovoltaics

Unlike the conventional 3 D perovskites (e.g., $MAPbI_3$ and $FAPbI_3$) that have been intensively studied in PVs since 2012, significantly less research effort has been placed on multidimensional perovskites in solar cell applications. The first demonstration of multidimensional perovskites in PSCs was reported by Smith et al. only in 2014.60 They presented the first single crystal structure

of a $n$ =3 perovskite, $(PEA)_2(MA)_2[Pb_3I_{10}]$ ($PEA^+$=phenethylammonium cation), derived from dark red crystals that were obtained by slow evaporation from a saturated solution. Although the pure $n$ =3 (where $n$ =the number of inorganic layers) perovskite can be grown from its precursor solution, the spin-coated thin film actually consisted of a mixture of different orders ($n$ =1, 2, 3, 4, and 5) in the perovskite film owing to the rapid self-assembly process. The multidimensional perovskite-based PVs exhibit overall PCE of 4.73 %, $J_{SC}$ of 6.72 mA $cm^{-2}$, $V_{OC}$ of 1.18 V, and FF of 0.60. The $V_{OC}$ value observed here is higher than for $MAPbI_3$-based solar cells. Despite the lower PCEs, this multidimensional perovskite displays high moisture resistance even after storage for 46 days under 52 % RH, whereas the $MAPbI_3$ thin film had turned from black to yellow under the same conditions (Figure 6 a).

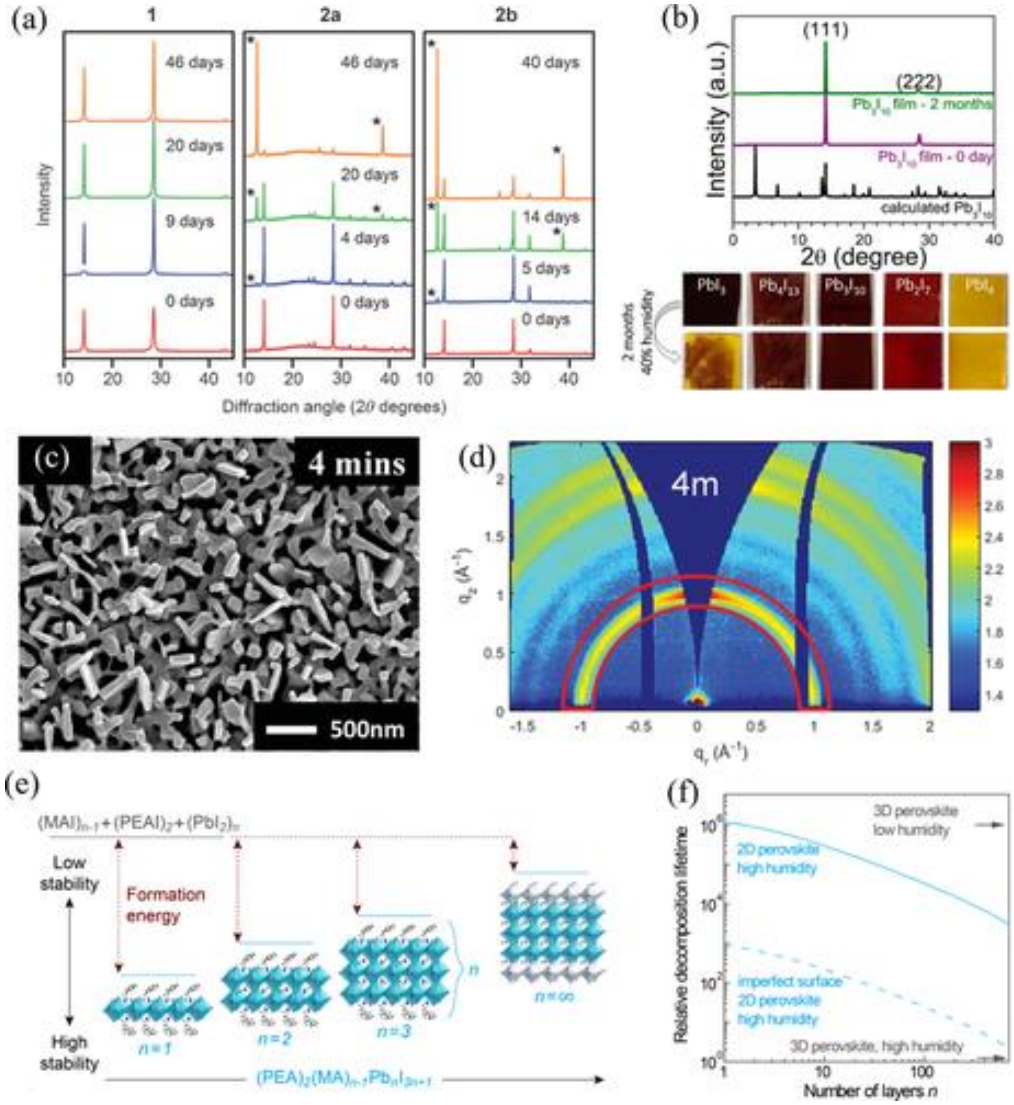


**Figure 6**. (a) pXRD patterns of films of $(PEA)_2(MA)_2Pb_3I_{10}$ (1), $MAPbI_3$ formed from $PbI_2$ (2 a), and $MAPbI_3$ formed from $PbCl_2$ (2 b), which were exposed to 52 % RH. Films of 2 a (15 min) and 2 b (80 min) were annealed at 100 °C prior to humidity exposure. Asterisks denote the major reflections from $PbI_2$. Adapted from Ref. 60. Copyright 2014 American Chemical Society. (b) XRD patterns of fresh and aged $(BA)_2(MA)_2Pb_3I_{10}$ films. The images below are the five different

perovskite films before and after exposure to humidity. Adapted from Ref. **61**. Copyright 2015 Wiley-VCH Verlag GmbH & Co. KGaA. (c) Top-view field-emission SEM images of nanostructures of $(IC_2H_4NH_3)_2(CH_3NH_3)_{n-1}Pb_nI_{3n+1}$ perovskites on top of a mesoporous $TiO_2$ layer from two different dipping durations in the sequential technique. (d) 2 D grazing-incidence wide-angle X-ray scattering (GIWAXS) data shown with a logarithmic false-color scale. The inhomogeneous intensity distribution of the ring at $q$ =1 $Å^{-1}$ for the 4 min sample indicates preferentially oriented crystals. Adapted from Ref. **59**. Copyright 2016 Wiley-VCH Verlag GmbH & Co. KGaA. (e) Unit cell structure and relative energetics of formation (i.e., stability) for $(C_8H_9NH_3)_2(CH_3NH_3)_{n-1}Pb_nI_{3n+1}$ with different values of $n$ (i.e., number of layers). (f) DFT calculations illustrating the relative formation energy of the 2 D perovskites containing different values of $n$ under different humidity environments. Adapted from Ref. **16d** Copyright 2012 American Chemical Society.

Almost a year later, a second set of PV devices based on multidimensional perovskites was reported by Cao et al.**61** A series of homologous perovskites, $(BA)_2(MA)_{n-1}PbI_{3n+1}$ ($BA^+$=*n*-butylammonium cation), were synthesized by introducing bulkier primary organic ammonium cations, thus confining the perovskites into a layered structure. Similar to the aforementioned report, the perovskite thin films reported also contained multiple orders of perovskites when they were prepared using a single step deposition method. The presence of mixeddimensional perovskites cannot be realistically avoided with the fast and low-temperature self-assembly processes currently utilized. The degree of orientation in these multidimensional perovskite films were far superior to the 3 D $MAPbI_3$ counterpart films indicating the potential for facile processing in both laboratory- and large-scale fabrication. However, the PCEs from these multidimensional perovskites were not satisfactory and the highest recorded value was only 4.02 % with $(BA)_2(MA)_2Pb_3I_{10}$ with high film stability over 2 months (Figure **6** b). Importantly, XRD analysis revealed that the lower dimensional perovskites ($n$ =1 and 2) tend to grow parallel to the substrate [along the (0 0 $k$ ) and (0 $k$ 0) plane], resulting in poorer charge transport in the (1 1 1) direction owing to the intercalated insulating organic cation layers.

Recently, our group implemented a nanostructuring approach to process multidimensional perovskites to create high-efficiency and stable PVs.**59** As the previous reports suggested that the insulating organic layers impeded charge transport in the layered perovskites, we addressed this issue by growing the perovskite perpendicular to the substrate. First, a pure 2 D perovskite ($n$ =1) was deposited by spin coating the precursor solution containing a stoichiometric ratio of lead iodide ($PbI_2$) and iodoethylammonium iodide ($IC_2H_4NH_3I$, IEAI). Subsequently, the substrate was immersed into a solution containing MAI for different dipping duration to increase the stacking order and convert it into a mixed-dimensional perovskite. Control of the dipping duration allowed us to tune the optical properties, direct the crystal growth perpendicular to the substrate, and hence improve the electrical properties (Figure 6 c and **6** d). This class of multidimensional perovskites exhibited good air stability and achieved over 9 % PCE with a mixed-cation approach.**59** More importantly, the PV devices degraded at much slower rates compared to those with $MAPbI_3$ without encapsulation under high RH (70–80 %).

To alleviate the inferior charge transport in multidimensional perovskite PVs, another method is to increase the number of stacked inorganic sheets to facilitate the charge transport within the device. For instance, Quan et al. demonstrated the utilization of higher order ($n$ =60)

multidimensional perovskites in PSCs, giving both high efficiency and stability (Figure 6 e and 6 f).[16d] The replacement of MAI with PEAI engenders higher stability owing to the latter's higher desorption energy and consequently slows down decomposition of the perovskite film. By periodically examining the absorbance, transient PL decay, and structure (by XRD) of the perovskite films, the authors verified that the multidimensional perovskites with intercalated $PEA^+$ cations possessed superior stability compared to the 3 D perovskites under ambient atmospheres, likely owing to the increased formation energy. The highefficiency $MAPbI_3$ PSC (16.6 %) deteriorated drastically to a PCE of less than 3 % over 8 weeks, whereas the multidimensional PVs remained stable at 11–13 % PCE.

Bulkier, hydrophobic organic cations in multidimensional perovskites could strain the surface Pb−I bonds and repel water molecules from reactive sites in the perovskites, hence promoting moisture resistance and prolonging the lifetime of the PSCs under ambient conditions.[62] In addition to the relatively small organic cations ($PEA^+$, $BA^+$, and $IEA^+$), polymeric organic cations are also potential candidates for preparing multidimensional perovskites with high air stability. Yao et al. demonstrated the effects of utilizing polyethylenimine hydriodide (PEI·HI) as intercalating organic cations in forming highly stable multidimensional perovskites (Figure 7 a).[63] High quality pinhole-free perovskites containing polymeric cations are readily formed after the spin-coating process, thus minimizing the shunt paths for the leakage current to offer opportunities to manufacture scalable perovskite PVs. The strong interaction between the polymeric organic–inorganic structures led to a lower $E_g$ compared to smaller molecular organic cations. Moreover, the polymeric cations also enhanced the charge transfer between the separated inorganic layers. The scaled up PSC devices (active area of 2.32 $cm^2$) with polymer-based multidimensional perovskites exhibited PCEs exceeding 8 % with excellent device lifetimes (Figure 7 b).

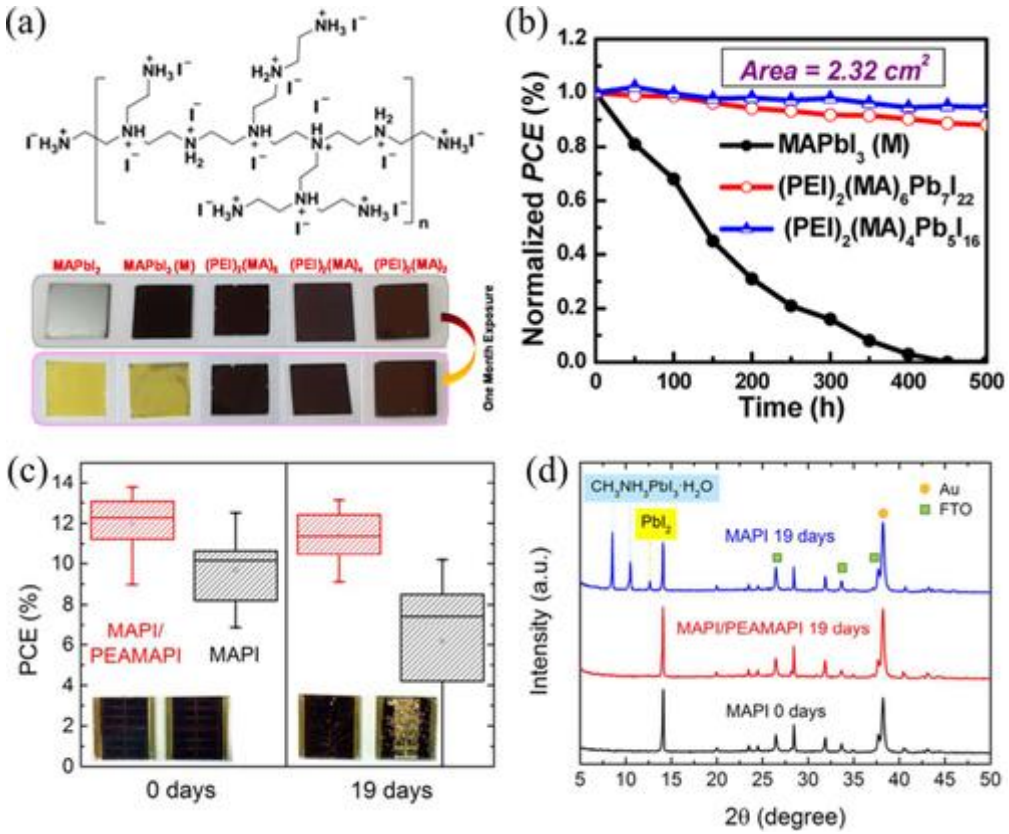


**Figure 7**. (a) Chemical structure of polyethylenimine hydriodide (PEI·HI) and the images of various perovskite films before and after exposure to 50 % RH. (b) Stability of unsealed cells under simulated solar illumination (AM 1.5 G; 100 mW cm$^{-2}$) during a shelf life investigation for 500 h. Adapted from Ref. **63**. Copyright 2016 American Chemical Society. (c) Device stability test at 75 % RH in air at room temperature for 19 days. Efficiency distribution for 20 $MAPbI_3/(PEA)_2(MA)_2Pb_3I_{10}$ and 20 $MAPbI_3$ devices before and after exposure to humidity. The insets show the corresponding photograph of a $MAPbI_3/(PEA)_2(MA)_2Pb_3I_{10}$ cell (left) compared to a $MAPbI_3$ control cell (right). (d) XRD patterns of an intact $MAPbI_3$ cell, a $MAPbI_3/(PEA)_2(MA)_2Pb_3I_{10}$ cell, and a $MAPbI_3$ cell upon exposure to moisture. Adapted from Ref. **64**. Copyright 2016 American Chemical Society.

Most recently, bilayer hybrid perovskites have been adopted in another strategy to promote the ambient stability of the existing high-efficiency PSCs. Generally, these kinds of bilayer hybrid structures contain high-efficiency 3 D perovskites on top of mesoporous $TiO_2$, while lower dimensional perovskites are placed on top to enhance the moisture resistance. Docampo and workers deposited layered perovskites, consisting of $PEA^+$ and $MA^+$ on top of $MAPbI_3$ and obtained PSCs with PCEs up to 16.8 % with increased $V_{OC}$ and FF (Figure 7 c).**64** The perovskites capped with lower dimensional perovskites exhibited average PCEs of 11.4 % after exposure to 19 days in 75 % RH (Figure 7 d), whereas pure 3 D perovskite devices only retained average PCEs of 6.1 %. It is also important to highlight that the energy level of the two perovskites layer in this bilayer approach have to be matched to facilitate the internal charge injection as well as the hole extraction for an efficient solar cell.

3.2 Challenges in multidimensional perovskites

Although lower dimensional perovskites have shown promising PV properties, especially stability under ambient atmospheric conditions, a few major challenges exist in this class of materials: poor interlayer charge transport, larger $E_g$, and high excitonic binding energies. The XRD diffraction patterns of 2 D perovskites typically give intense (0 0 L) reflections, indicating a preferred growing direction parallel to the substrate (Figure 8 a).[65] This preferential growth among 2 D perovskites results in poor charge transport between the inorganic layers in conventional perovskite PVs, but is suitable for optoelectronics in which the current flow direction should be parallel to the inorganic sheets in lower dimensional perovskites. As an example, Kagan et al. demonstrated a perovskite-based field-effect transistor using $(C_6H_5C_2H_4NH_3)_2SnI_4$ perovskite and measured a mobility of 0.61 $cm^2\ V^{-1}\ S^{-1}$, which was comparable to the performance in amorphous Si devices (Figure 8 b).[66]

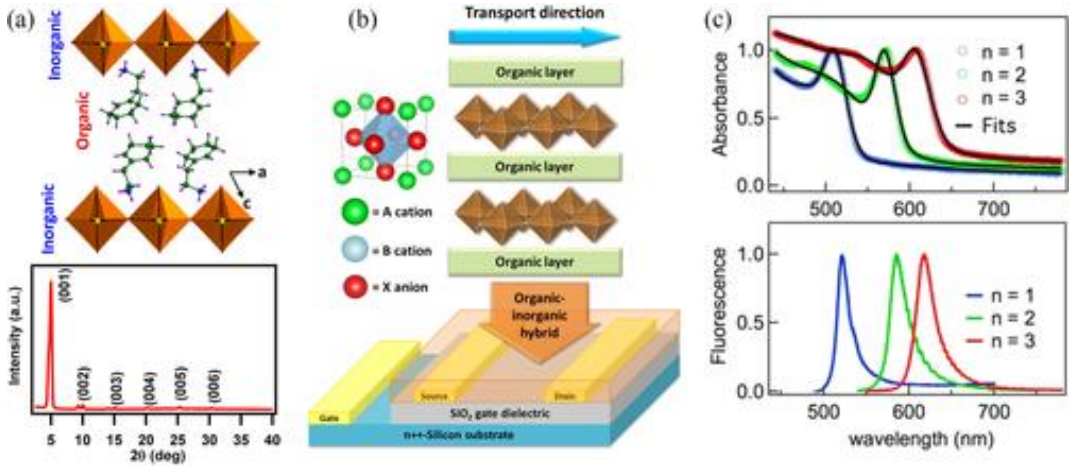


**Figure 8**. (a) Crystal structure of 2 D perovskite $(C_6H_9C_2H_4NH_3)_2PbI_4$ and the XRD pattern of a thin film revealing a 2 D-layered arrangement. Adapted from Ref. 65. Copyright 2015 American Chemical Society. (b) Reproduced schematic of a thin-film field-effect transistor device structure having a layered organic–inorganic perovskite as the semiconducting channel. Adapted from Ref. 66 with permission from the American Association for the Advancement of Science. (c) Room temperature absorption (upper, color circles: data points; black curves: fits) and fluorescence (lower) spectra of 2 D lead halide perovskite quantum well samples: $(C_4H_9NH_3I_2)_2(CH_3NH_3I)_{n-1}(PbI_2)_n$, $n$ =1, 2, 3. Adapted from Ref. 68. Copyright 2015 American Chemical Society.

According to the Shockley–Queisser limit, the optimum $E_g$ for a light absorber should be 1.1 eV to achieve up to 34 % PCE.[67] However, in lower dimensional perovskites, the band gap will be increased as the dimensionality is reduced (Figure 8 c).[68] Another detrimental factor in 2 D perovskites is the higher excitonic binding energy, which hinders charge separation and can lead to poorer PV performances. In 3 D perovskites, free charges rather than excitons are predominantly generated during PV operation because the binding energies are low. Unlike 3 D perovskites however, 2 D or lower dimensional perovskites often possess stronger exciton binding energies owing to the dielectric confinement effect, which can lead to exciton recombination and therefore reduced charge collection.[69] Additional complications could arise from excitonic traps in 2 D perovskites $[(C_4H_9NH_3)_2PbI_4]$, which are evident from sub-$E_g$ PL.[70] Lowering the dimensionality could result in reduced deformation energy and hence more prevalent self-trapping, consistent with

a prior theoretical study where ionic point defects were calculated to arise from the low lattice energy among halide perovskites.[70, 71] In Table 1, we have summarized the relationship between the dimensionality of perovskites and the resonance energies, the binding energies of the lowest-energy excitons, and the band gap energies.

**Table 1.** Resonance energies ($E_{res}$), binding energies ($E_b$) of the lowest-energy excitons, and the band gap energy ($E_g$) in $(C_6H_{13}NH_3)_2(CH_3NH_3)_{m-1}Pb_mI_{3m-1}$ at 5 K. Adapted from Ref. [69]. Copyright 2004 Elsevier Ltd.

| Crystals | *m* | $E_{res}$ [eV] | $E_b$ [eV] | $E_g$ [eV] |
|---|---|---|---|---|
| monolayer | 1 | 2.34 | 361 | 2.70 |
| bilayer | 2 | 2.14 | 260 | 2.40 |
| trilayer | 3 | 2.02 | 150 | 2.17 |
| tetralayer | 4 | 1.92 | 100 | 2.02 |
| 3 D | ∞ | 1.65 | 50 | 1.70 |

## 4 Perspective and Outlook

Although multidimensional perovskites seem to be promising candidates in delivering high PCEs with reasonably high ambient stabilities, the charge transport within the absorber layer still remains a concern in achieving stable and highly efficient PSCs. This is exacerbated by the tendency of the 2 D perovskites to crystallize with the inorganic high mobility planes perpendicular to the direction of transport in solar cells. Recently hot-casting of Ruddlesden–Popper multidimensional perovskites $(BA)_2(MA)_{n-1}Pb_nI_{3n+1}$ produced near-single-crystalline quality films in which the inorganic crystallographic planes have a preferential out-of-plane orientation that facilitate efficient charge transport. These materials in PV devices exhibited high PCEs of 12.52 % without hysteresis and showed improved stability characteristics.[72] As process control during hot-casting is challenging, this may not be a widely scalable technique to improve charge transport. However this work clearly shows the utility of multidimensional perovskites. Here, we propose two approaches for PSCs that would maintain charge-transport properties while concurrently enhancing the stability.

### 4.1 π-Conjugated organic cations

Besides the aliphatic alkylammonium cations that have been incorporated into devices recently, we identify redox-active and potentially photo-active π-conjugated organic cations as attractive alternatives. These π-electron rich cations can offer additional channels to improve interlayer charge transport and extraction. In the late 1990s, Mitzi and others have introduced 2-thienylmethylammonium, bithiophene mono and diammonium, and even quaterthiophene diammonium cations into 2 D lead and bismuth halide perovskites.[73] The potential of 2 D metal halide perovskites in optoelectronics applications, such as non-linear optical materials and light-emitting devices, had been recognized then, but progress was hampered by the dramatic fall in electroluminescence and PL efficiencies when the perovskites were raised from liquid $N_2$ temperatures to room temperature. Consequently, the PL and redox-active thiophene-containing organic ammonium cations were introduced between the 2 D Pb and Bi halides, several

of which were crystallographically characterized.[73] Interestingly, the perovskites containing mono and bithiophene ammonium cations appear to have quenched PL at room temperature, but higher dark currents in applied electric fields.[73a, 73] On the other hand, perovskites with quaterthiophene ammonium cations exhibit high efficiency electroluminescence under ambient conditions with turn-on voltages as low as 5.5 V, with the luminescence originating from the quaterthiophene motif.[55, 73b] The perovskite layers were up to 3 μm thick, suggesting that charge transport remained remarkably effective between the inorganic sheets.[55, 73b]

In a revitalization of this field, a small number of new redox- and photo-active organic cations have lately been introduced into the metal halide perovskites. For most cases, energy transfer from the perovskite excitons to the organic chromophore occurred, resulting in enhanced emission arising from the organic moiety.[74] However, Jemli et al. partially incorporated 2,3-naphthalimide-ethylammonium (NAAB) into $(PEA)_2PbBr_4$ and observed improved PL behavior that did not merely originate from the NAAB emission.[75] They proposed that judicious choice of the organic cation by matching the HOMO–LUMO gap of NAAB to the exciton $E_g$ of $(PEA)_2PbBr_4$ led to nearresonance, which increased quantum yields of radiative relaxation. Maughan et al. also attempted to improve charge-transport properties of Sn and Pb iodides with the use of the redox-active tropylium cations.[76] Although optical absorption spectra and DFT calculations suggested that there was increased charge transfer and electronic coupling between $I^-$ and the tropylium cations, the low conductivity of the 1 D face-sharing lead iodide chains inhibited the carrier mobility in these materials overall.[76] Nonetheless, these efforts indicate that appropriate selection of organic cations can strongly influence the optoelectronic properties of the resultant perovskites. More recently, tetrathiafulvalene (TTF) radical cations have been introduced into 2 D lead halide nanosheets to produce crystalline $(TTF)Pb_2I_5$ materials.[77] TTF radical cations had previously been employed to create novel metallic and magnetic materials. The $(TTF)Pb_2I_5$ displayed room temperature conductivity in excess of 0.01 S $cm^{-1}$, which is about four orders of magnitude greater than the parent TTF halide salts.[77] Although these 2 D perovskites typically exhibit larger $E_g$ and cannot be directly utilized for PSCs, we believe that an astute selection of redox- and photo-active π-conjugated organic cations into multidimensional metal halide perovskites can dramatically improve the charge transport and extraction properties in devices. Their introduction at the interfaces with the charge-extraction layers can be especially beneficial, as discussed in the following sections.

### 4.2 Gradient multidimensional perovskites

As highlighted previously, moisture-induced degradation could be the root cause for the instability of most PSCs. Hence, an increase in hydrophobicity on the perovskite surface and strengthening the interactions within the perovskite layer become crucial. During investigations on the effects of water on PSCs, DFT calculations indicated that the conduction band minimum (CBM) of $MAPBI_3$ was localized around the fivecoordinate surface Pb atoms, which facilitated Lewis-base interactions between water and the surface CBM of the perovskite (Figure 9 a and [9] b).[62] When $MA^+$ was replaced by a bulkier tetramethylammonium cation ($TMA^+$), the surface I atoms shifted above the surface Pb atoms, which combined with the hydrophobicity of the ammonium cations to make the surface more water-repellent (Figure [9] c). Slightly bulkier tetraethylammonium ($TEA^+$) cations led to even more significant changes to the surface I atoms and hindered water adsorption to the surface Pb sites even more effectively. This strategy can also be considered as a gradient multidimensional approach, where the top surface is converted into a very thin 2 D/mixed

perovskite, while the layer underneath retains its 3 D structure. Consequently, the overall unit possesses enhanced moisture stability and preserves its high PCE.

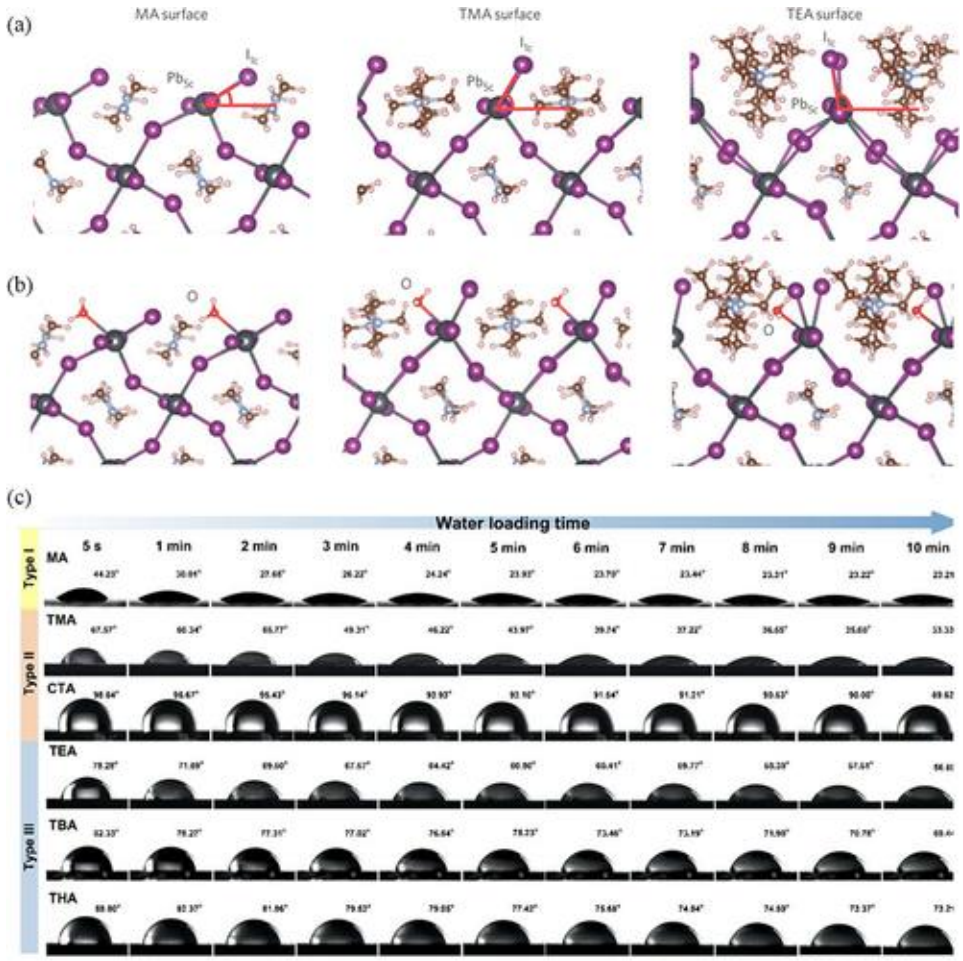


**Figure 9**. (a) Side views of the computationally optimized geometries of the (1 0 0) surfaces of MA, TMA, and TEA samples. (b) Calculated atomic structures (side view) of different (1 0 0) surfaces with molecularly adsorbed water. The red angles between the surface $Pb_{5c}$–$I_{1c}$ bonds and the (1 0 0) surface reflect the steric hindrance of the water adsorption on the reactive $Pb_{5c}$ sites on different surfaces. Pb, I, C, N, O, and H atoms have been represented by spheres in grey, purple, brown, blue, red, and pink, respectively. (c) Representative photographs showing the water contact angles of perovskite films with different surfaces. Although bulk perovskite readily absorbs water, its wetting ability can indeed be regulated and considerably suppressed when functionalized with certain ammonium cations on the surface. Adapted from Ref. **62** with permission from the Nature Publishing Group.

Chemical additives could co-crystallize with $MAPbI_3$ to form passivated 3 D perovskites that have longer-term stability. They can be considered to be near the limits of mixed-dimensional perovskites (*n* almost ∞) and the additives appear to enhance the quality or counteract undesirable properties to improve PSC performance. Grätzel and coworkers used a phosphonic acid ammonium cation as an additive in perovskites to crosslink neighboring perovskite grains through strong hydrogen bonding between the $-PO(OH)_2$ and $-NH_3^+$ terminal groups (Figure **10** a).**78** The

bifunctional butylphosphonic acid 4-ammonium chloride (4-ABPACl) facilitated the smooth growth of perovskite crystals on the mesoporous scaffold and, more importantly, improved the moisture stability compared to pristine 3 D perovskites. Molecular engineering with functional chemical additives can offer a new and effective solution to modulate the photophysical properties of metal halide perovskites for commercial fabrication. Likewise, Bi et al. incorporated small amounts of hydrophobic fluorinated ammonium cations, such as trifluoroethylammonium iodide ($CF_3CH_2NH_3I$, FEAI) into their PV devices to improve the morphology of the perovskite without increasing the $E_g$ and exciton binding energy, which would reduce the light harvesting capability.[79] With a small quantity of FEAI in $MAPbI_3$, the PCE was improved and the water resistance was enhanced (Figure 10 b), resulting in devices that were stable up to 4 months.

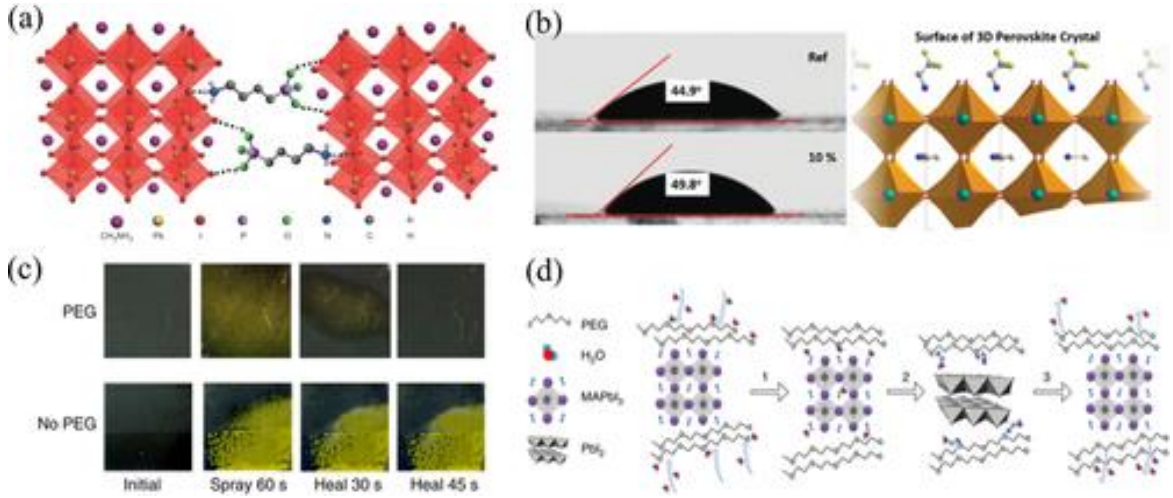


**Figure 10**. (a) Illustration of two neighboring grain structures in which the methylammonium groups are shown as purple spheres for clarity, and the $PbI_6^{4-}$ octahedra are shown in red, crosslinked by hydrogen-bonding interactions (O−H···I and N−H···I) between the phosphonic acid [$-PO(OH)_2$] and the ammonium ($-NH_3^+$) end groups of 4-ABPACl with the iodide from the iodoplumbate complex. Adapted from Ref. [78] with permission from the Nature Publishing Group. (b) The static contact angles of the pristine perovskite film and the perovskite film with 10 % FEAI with deionized water. The Figure (right) shows the model of the FEAI intercalating on the crystal surface of a 3 D perovskite $MAPbI_3$. Atom colors: Pb=turquoise, I=purple, N=blue, C=gray, and F=yellow. Hydrogen atoms have been omitted for clarity. Adapted from Ref. [79]. Copyright 2015 Wiley-VCH Verlag GmbH & Co. KGaA. (c) Photographs of perovskite films with and without PEG showing the evolution of color after exposure to water for 60 s and storage in ambient air for 45 s. (d) Diagram to show mechanisms for the self-healing properties in polymer-scaffold PSCs: (1) water absorbed on perovskite, (2) perovskite hydrolysis into $PbI_2$ and $MAI{\cdot}H_2O$ by water, and (3) spatially constrained MAI (by PEG) react with nearby $PbI_2$ to form perovskite again after water evaporates. PEG has a strong interaction with MAI, preventing it from evaporating; subsequently MAI and $PbI_2$ react in situ to form $MAPbI_3$ again after the film has been removed from the vapor source. Adapted from Ref. [80] with permission from the Nature Publishing Group.

Recently, Zhao et al. reported an alternative, novel PSC architecture based on an insulating polymer (polyethylene glycol, PEG) scaffold structure, which displayed remarkably stable device performance in highly humid environments (70 % RH).[80] The insulating PEG scaffold stabilized the perovskite PVs owing to its strong hygroscopicity. With the PEG scaffold, the PSC retained

83 % of its original efficiency under continuous light illumination. More interestingly, PEG–perovskite devices demonstrated self-healing behavior and moisture resistance upon exposure to water vapor. The PEG-containing perovskite film initially turned yellow when exposed to water vapor, but recovered its black color in about 45 s (Figure 10 c). However, perovskite films without PEG turned yellow irreversibly after exposure to the water vapor. Owing to the strong hydrogen-bonding interaction between the MAI and PEG, the MAI molecules were anchored to the nearby PEG molecules, preventing the escape of MAI salts from the perovskite film. The rapid decomposition–regeneration mechanism has been depicted in Figure 10 d.

The above mentioned developments in photo-absorber design needs to be combined with device concepts and interfacial layers that have shown promising stability enhancements. The introduction of interfacial modifiers (e.g., CsBr, $Sb_2S_3$, CdS) between the electron-selective contact and the perovskite layer may turn out to be necessary.[81] Alternative mesostructured metal oxide scaffolds, such as $Al_2O_3$,[46], [82] $SnO_2$,[83] ZnO,[84] $NiO_x$,[85] and NiMgLiO[86] that may show more UV resistance, and additive-free hole-transporting layers[87] that will not cause deleterious effects on the perovskite layer would need to be carefully evaluated. An architecture that incorporates many of the above factors was demonstrated by Mei et al. who utilized a device architecture consisting of a combination of mesoporous layers of $TiO_2$, $ZrO_2$, and conducting carbon, while the perovskite crystallized in the mesoporous device.[88] Extraordinary device stability (1000 h under AM 1.5 G illumination) could be a result of the presence of the mesoporous $ZrO_2$ and carbon layers, which restrict the direct contact of moisture to the perovskite and hence prolonged the lifetime of the devices. After this seminal publication, several groups have published reports on carbon-based PSCs with enhanced PCEs.[89] Apart from enhancing the stability of PSCs by material and interfacial engineering, a simple and efficient encapsulation technique can also be incorporated in perovskite PVs. These have included ALD deposited layers,[82b] $Cr_2O_3$[90] and polymeric films, like Teflon[91] and more conventional encapsulants.[92]

## 5 Summary

In the past few years, perovskite PVs have shown unprecedented rapid advancement and the PCEs have exceeded 20 % through optimizing the interlayers and device configuration. To allow the perovskite PVs to be commercialized, their ambient instability is one of the main obstacles that has to be first overcome in the laboratory. Thus, enhancing the intrinsic ambient stability of perovskites has emerged as one of the top research topics in the community. We believe that a multidimensional approach is one of the most promising strategies to improve the stability of perovskites. This review has highlighted the sources of instability in conventional 3 D perovskites, including water intercalation, ion migration, and thermal decomposition. The hygroscopic nature of perovskites, which arises because the inorganic layers are held together through electrostatic attraction between cationic and anionic species, allows water molecules to intercalate easily, and subsequently results in dissociation into ammonium salts and lead halide residues. Furthermore, vacancies in the perovskites will accommodate ionic migration and phase separation, which leads to compromised device performances under continuous illumination during full operation. The cationic and halide components in the perovskites can also be liberated by applying moderately high temperatures, causing thermal decomposition and deterioration in device performances.

As discussed in the previous section, there are potential issues in 3 D $MAPbI_3$ perovskite that could lead to the instability of PCSs: thermal degradation, ion migration, and phase transition. With the

incorporation of larger organic cations, mixed-dimensional perovskites could also be chemically stable at higher temperatures owing to the lower volatility of the larger ammonium cations as compared to $MA^+$. In addition, the organic cations can be rationally designed to have extra bonding (hydrogen or halogen bonding) to the terminal halide of the $PbI_6^{4-}$ octahedra for a better stability. Another potential advantage of using larger organic cations in mixed-dimensional perovskites is its reduced ionic motion. Both $MA^+$ and $FA^+$ have low migration barriers[28c] and could possibly move under an applied bias. Therefore, replacing them with larger organic cations (in mixed-dimensional perovskites) could potentially suppress the hysteresis and also avoid the lattice distortion and contraction, which could be caused by cation migrations, leading to more stable perovskites.

Multidimensional perovskites have become promising candidates to surmount the challenges of ambient instability in conventional 3 D perovskites. As compared to the pure 2 D perovskites, multidimensional perovskites typically possess more ideal $E_g$ and better charge transport for PV applications. More importantly, the conductivity in the vertical direction (normal to the charge-extraction layers in a conventional device configuration) can be higher in mixed multidimensional perovskites because the pure 2 D perovskites tend to crystalize parallel to the substrate. Another main advantage of mixed multidimensional perovskites is the lower exciton-binding energy compared to pure 2 D perovskites, which is essential for PVs so that the charges can be separated easily. With multidimensional perovskites, PCEs of more than 16 % have been achieved with remarkable long-term stability.[64] Interfacial and materials engineering will undoubtedly significantly enhance their stability in ambient atmospheric conditions. For example, partial substitution of $MA^+$ with other larger, hydrophobic organic cations or polymeric cations has proven as one of the most successful ways to improve the stability of perovskites. Combining 3 D and 2 D perovskites in multidimensional perovskites has provided hybrid PVs with improvements in efficiency and stability, whereas interfacial modifications and functionalization can further increase the ambient stability. In addition, chemical additives (larger organic ammonium salts) for multidimensional perovskites remarkably enhance the long-term stability by repelling water from the surface of multidimensional perovskites. In this Review, we have highlighted some of the potential device encapsulation methods that can elevate the stability of multidimensional PVs.

We anticipate that tremendous research efforts will be invested in multidimensional perovskites to develop higher PCEs and long-term stability. Consequently, multidimensional perovskites also offer the opportunity to scale up manufacturing processes, such as screen-printing, roll-to-roll slot die-coating, or ink-jet printing technologies, owing to the improved ambient stability and highly crystalline properties of future perovskites. With the meteoric progress in perovskite PVs, we believe that it will be one of the main challengers to the market-dominant Si-based PVs.

**Acknowledgements**
The authors would like to acknowledge Prof. Subodh Mhaisalkar for valuable discussions. The funding from Singapore National Research Foundation through the Competitive Research Program: NRF-CRP14–2014–03 as well as the Singapore-Berkeley Research Initiative for Sustainable Energy (SinBeRISE) CREATE programme is acknowledged. Support from NTU-A*STAR Silicon Technologies Centre of Excellence under the program grant No. 112 3510 0003 is also acknowledged. H.S.S. is supported by an MOE Tier 1 grant (M4011144), the Nanyang

Assistant Professorship (M4081154), and a NTU start-up grant (M4081012). H.S.S. also thanks the support from the Solar Fuels Laboratory at NTU.

References

1] D. Kim, K. K. Sakimoto, D. C. Hong, P. D. Yang, Angew.Chem. Int. Ed. 2015, 54,3259 –3266; Angew.Chem. 2015, 127,3309 –3316.

[2] N. S. Lewis, Science 2016, 351,353.

[3] M. Sessolo, H. J. Bolink, Science 2015, 350,917–917.

[4] A. Kojima, K. Teshima, Y. Shirai, T. Miyasaka, J. Am. Chem. Soc. 2009, 131, 6050–6051.

[5] W. S. Yang, J. H. Noh,N.J.Jeon, Y. C. Kim, S. Ryu, J. Seo, S. I. Seok, Science 2015, 348,1234 –1237.

[6] H. P. Zhou,Q.Chen,G.Li, S. Luo, T. B. Song, H. S. Duan, Z. R. Hong, J. B. You, Y. S. Liu, Y. Yang, Science 2014, 345,542–546.

[7] C. Bi, Q. Wang, Y. C. Shao, Y. B. Yuan, Z. G. Xiao, J. S. Huang, Nat. Commun. 2015, 6,7747.

[8] Q. Q. Lin, A. Armin, P. L. Burn, P. Meredith, Acc.Chem. Res. 2016, 49, 545–553.

[9] D. P. McMeekin, G. Sadoughi, W. Rehman,G.E.Eperon, M. Saliba, M. T. Horantner,A.Haghighirad, N. Sakai, L. Korte, B. Rech,M.B.Johnston, L. M. Herz, H. J. Snaith, Science 2016, 351,151 –155.

[10] P. Docampo, T. Bein, Acc. Chem. Res. 2016, 49,339 –346.

[11] a) Z. K. Tan, R. S. Moghaddam,M.L.Lai, P. Docampo, R. Higler,F.Deschler,M.Price, A. Sadhanala, L. M. Pazos, D. Credgington, F. Hanusch, T. Bein, H.J. Snaith, R. H. Friend, Nat. Nanotechnol. 2014, 9,687–692; b) N.Yantara, S. Bhaumik, F. Yan, D. Sabba, H. A. Dewi, N. Mathews,P.P.Boix, H. V. Demir,S.Mhaisalkar, J. Phys. Chem.Lett. 2015, 6,4360 –4364; c) E. R. Dohner,E.T.Hoke, H. I. Karunadasa, J. Am. Chem. Soc. 2014, 136, 1718–1721; d) E.R.Dohner,A.Jaffe, L. R. Bradshaw,H.I.Karunadasa, J. Am. Chem. Soc. 2014, 136,13154–13157.

[12] a) G. Xing, N. Mathews, S. S. Lim, N. Yantara, X. Liu, D. Sabba, M. Gratzel, S. Mhaisalkar, T. C. Sum, Nat. Mater. 2014, 13,476 –480; b)H.M. Zhu, Y. P. Fu, F. Meng, X. X. Wu, Z. Z. Gong, Q. Ding, M. V. Gustafsson,M.T. Trinh, S. Jin, X. Y. Zhu, Nat. Mater. 2015, 14,636–642;c)Y.J.Li, Y. C. Lv, C. L. Zou, W. Zhang,J.N.Yao, Y. S. Zhao, J. Am. Chem. Soc. 2016, 13 8, 2122–2125.

[13] a) J. Y. Liu, Y. Z. Xue, Z. Y. Wang, Z. Q. Xu, C. X. Zheng, B. Weber,J.C. Song, Y. S. Wang, Y. R. Lu, Y. P. Zhang, Q. L. Bao, ACS Nano 2016, 10, 3536–3542;b)Y.S.Wang, Y. P. Zhang,Y.Lu, W. D. Xu, H. R. Mu, C. Y. Chen, H. Qiao, J. C. Song,S.J.Li, B. Q. Sun, Y. B. Cheng, Q. L. Bao, Adv Opt Mater 2015, 3,1389 –1396;c)H.Deng, X. K. Yang, D. D. Dong, B. Li,

D. Yang, S. J. Yuan, K. K. Qiao, Y. B. Cheng, J. Tang,H.S.Song, Nano Lett. 2015, 15,7963–7969;d)L.Su, Z. X. Zhao, H. Y. Li,J.Yuan, Z. L. Wang, G. Z. Cao, G. Zhu, ACS Nano 2015, 9,11310 –11316.

[14] X. Y. Chin, D. Cortecchia, J. Yin, A. Bruno,C.Soci, Nat. Commun. 2015, 6, 7383.

[15] a) G. Walters, B. R. Sutherland, S. Hoogland, D. Shi, R. Comin, D. P. Sellan, O. M. Bake,E.H.Sargent, ACS Nano 2015, 9,9340–9346; b) R.Zhang, J. D. Fan, X. Zhang, H. H. Yu,H.J.Zhang, Y. H. Mai, T. X. Xu, J. Y. Wang, H. J. Snaith, ACS Photonics 2016, 3,371–377;c)Y.Wang, X. M. Li, X. Zhao, L. Xiao, H. B. Zeng, H. D. Sun, Nano Lett. 2016, 16,448 –453.

[16] a) Y. Yuan, J. Huang, Acc. Chem. Res. 2016, 49,286–293;b)K.W.Tan, D. T. Moore, M. Saliba, H. Sai, L. A. Estroff, T. Hanrath, H. J. Snaith, U. Wiesner, ACS Nano 2014, 8,4730 –4739;c) M.Wang, S. Lin, Adv.Funct. Mater. 2016,inpress, DOI:10.1002/adfm.2016 00284;d) L. N. Quan, M. Yuan, R. Comin, O. Voznyy,E.M.Beauregar d, S. Hoogland, A. Buin, A. R. Kirmani, K. Zhao, A. Amassian, D. H. Kim, E. H. Sargent, J. Am. Chem. Soc. 2016, 138,2649 –2655;e)N.Klein-Kedem, D. Cahen, G. Hodes, Acc. Chem. Res. 2016, 49,347 –354.

[17] a) D. Cortecchia, H. A. Dewi, J. Yin, A. Bruno, S. Chen, T. Baikie, P. P. Boix, M. Gratzel, S. Mhaisalkar,C.Soci, N. Mathews, Inorg. Chem. 2016, 55, 1044–1052;b)M.H.Kumar,S.Dharani, W. L. Leong, P. P. Boix, R. R. Prabhakar,T.Baikie, C. Shi,H.Ding, R. Ramesh, M. Asta, M. Gr-tzel, S. G. Mhaisalkar,N.Mathews, Adv.Mater. 2014, 26,7122 –7127;c)T.Krishnamoorthy,H.Ding, C. Yan, W. L. Leong, T. Baikie, Z. Y. Zhang, M. Sherburne, S. Li, M. Asta, N. Mathews,S.G.Mhaisalkar, J. Mater. Chem. A2015, 3,23829–23832.

[18] G. D. Niu, X. D. Guo, L. D. Wang, J. Mater.Chem. A 2015, 3,8970 –8980.

[19] a) K. K. Bass, R. E. McAnally,S.L.Zhou, P. I. Djurovich, M. E. Thompson,B. C. Melot, Chem. Commun. 2014, 50,15819 –15822;b)G.E.Eperon,S. N. Habisreutinger,T.Leijtens, B. J. Bruijnaers, J. J. van Franeker,D.W.Dequilettes, S. Pathak, R. J. Sutton, G. Grancini, D. S. Ginger,R.A.J.Jans-sen, A. Petrozza,H.J.Snaith, ACS Nano 2015, 9,9380 –9393.

[20] a) J. A. Christians, P. A. Miranda Herrera, P. V. Kamat, J. Am. Chem. Soc.2015, 137,1530 –1538;b)Y.Guo, K. Shoyama, W. Sato, Y. Matsuo, K.Inoue,K.Harano ,C.Liu,H.Tanaka, E. Nakamura, J. Am. Chem.Soc.2015, 137,15907–15914; c) J. S. Manser,M.I.Saidaminov, J. A. Christi-ans, O. M. Bakr,P.V.Kamat, Acc.Chem. Res. 2016, 49,330 –338;d)B.R.Vincent, K. N. Robertson, T. S. Cameron, O. Knop, Can. J. Chem. 1987, 65,1042–1046;e)J.L.Yang, B. D. Siempelkamp, D. Y. Liu, T. L. Kelly, ACSNano 2015, 9,1955 –1963.

[21] A. M. A. Leguy,Y.Hu, M. Campoy-Quiles, M. I. Alonso, O. J. Weber,P.Azarhoosh, M. van Schilfgaarde, M. T. Weller,T.Bein, J. Nelson,P.Do-campo,P.R.F.Barnes, Chem.Mater. 2015, 27,3397 –3407.

[22] A. Wakamiya, M. Endo,T.Sasamori, N. Tokitoh,Y.Ogomi, S. Hayase,Y.Murata, Chem. Lett. 2014, 43,711 –713.

[23] J. M. Frost, K. T. Butler,F.Brivio, C. H. Hendon, M. van Schilfgaarde,A.Walsh, Nano Lett. 2014 , 14,2584 –2590.

[24] a) A. Amat, E. Mosconi,E.Ronca,C.Quarti, P. Umari, M. K. Nazeeruddin,M. Gr-tzel, F. De Angelis, Nano Lett. 2014, 14,3608 –3616;b)N.J.Jeon,J. H. Noh, W. S. Yang, Y. C. Kim, S. Ryu,J.Seo,S.I.Seok, Nature 2015,517,476–480;c)M.Saliba, T. Matsui, J.-Y.Seo,K.Domanski, J.-P.Correa-Baena,M.K.Nazeeruddin, S. M. Zakeeruddin, W. Tress, A. Abate, A. Hag-feldt, M. Gr-tzel, EnergyEnviron. Sci. 2016, 9,1989 –1997;d)G.E.Eperon, C. E. Beck,H.J.Snaith, Mater. Horiz. 2016, 3,63–71.

[25] a) Q. A. Akkerman, V. D'Innocenzo,S.Accornero,A.Scarpellini, A. Petroz-za, M. Prato, L. Manna, J. Am. Chem. Soc. 2015, 137,10276–10281;b) D. M. Jang, K. Park, D. H. Kim, J. Park, F. Shojaei, H. S. Kang,J.-P.Ahn,J. W. Lee, J. K. Song, Nano Lett. 2015, 15,5191 –5199;c)G.Nedelcu, L.Protesescu, S. Yakunin,M.I.Bodnarchuk, M. J. Grotevent, M. V. Kovalen-ko, NanoLett. 2015, 15,5635–5640;d)A.B.Wong, M. Lai,S.W.Eaton,Y. Yu,E.Lin, L. Dou, A. Fu, P. Yang, NanoLett. 2015, 15,5519 –5524.

[26] a) J. Mizusaki, K. Arai, K. Fueki, Solid State Ionics 1983, 11,203 –211;b) D. A. Egger,A.M.Rappe, L. Kronik, Acc. Chem. Res. 2016, 49,573 –581.

[27] D. A. Egger,L.Kronik, A. M. Rappe, Angew.Chem. Int. Ed. 2015, 54,12437–12441; Angew.Chem. 2015, 127,12614 –12618.

[28] a) J. M. Azpiroz, E. Mosconi,J.Bisquert, F. De Angelis, Energy Environ. Sci.2015, 8,2118–2127;b)C.Eames, J. M. Frost, P. R. F. Barnes, B. C.O'Regan,A.Walsh, M. S. Islam, Nat. Commun. 2015, 6,7497;c)J.Har-uyama, K. Sodeyama, L. Han, Y. Tateyama, J. Am. Chem. Soc. 2015, 137,10048–10051; d) S. A. Kulkarni, T. Baikie, P. P. Boix,N.Yantara, N. Math-ews, S. Mhaisalkar, J. Mater.Chem.A2014, 2,9221 –9225.

[29] E. T. Hoke, D. J. Slotcavage, E. R. Dohner,A.R.Bowring, H. I. Karunadasa,M. D. McGehee, Chem. Sci. 2015, 6,613 –617.

[30] T.-Y.Yang,G.Gregori, N. Pellet, M. Gr-tzel, J. Maier, Angew.Chem. Int. Ed.2015, 54,7905 –7910; Angew.Chem. 2015, 127,8016 –8021.

[31] D. W. deQuilettes, W. Zhang, V. M. Burlakov,D.J.Graham, T. Leijtens, A.Osherov,V.Bulovic, H. J. Snaith,D.S.Ginger,S.D.Stranks, Nat.Commun. 2016, 7,11683.

[32] Y. Yuan, Q. Wang, Y. Shao,H.Lu, T. Li, A. Gruverman, J. Huang, Adv.EnergyMater. 2016, 6,1501803.

[33] Y. B. Yuan, J. Chae, Y. C. Shao,Q.Wang, Z. G. Xiao, A. Centrone,J.S.Huang, Adv.Energy Mater. 2015, 5,1500615.

[34] a) A. Mattoni,A.Filippetti, M. I. Saba, C. Caddeo, P. Delugas, J. Phys.Chem. Lett. 2016, 7,529–535;b)A.Pisoni, J. Jacimovic, O. S. Barisic, M.Spina, R. Gaal, L. Forro,E.Horvath, J. Phys. Chem. Lett. 2014, 5,2488 –2492.

[35] A. Dualeh, P. Gao, S. I. Seok, M. K. Nazeeruddin, M. Gr-tzel, Chem.Mater.2014, 26,6160 – 6164.

[36] a) W. L. Leong, Z.-E. Ooi, D. Sabba, C. Yi,S.M.Zakeeruddin, M. Gr-tzel,J. M. Gordon, E. A. Katz, N. Mathews, Adv.Mater. 2016, 28,2439 –2445;b) N. Yantara, F. Yanan, C. Shi, H. A. Dewi, P. P. Boix, S. G. Mhaisalkar,N.Mathews, Chem.Mater. 2015, 27,2309 –2314.

[37] N. K. Noel, A. Abate, S. D. Stranks, E. S. Parrott, V. M. Burlakov,A.Goriely,H. J. Snaith, ACS Nano 2014, 8,9815 –9821.

[38] A. Abate, M. Saliba, D. J. Hollman,S.D.Stranks, K. Wojciechowski, R.Avolio,G.Grancini, A. Petrozza, H. J. Snaith, Nano Lett. 2014, 14,3247 –3254.

[39] T. Baikie, Y. Fang, J. M. Kadro, M. Schreyer,F.Wei, S. G. Mhaisalkar,M.Gr-tzel, T. J. White, J. Mater.Chem.A2013, 1,5628 –5641.

[40] a) N. Pellet, P. Gao,G.Gregori, T. Y. Yang, M. K. Nazeeruddin,J.Maier,M.Gr-tzel, Angew.Chem. Int. Ed. 2014, 53,3151 –3157; Angew.Chem.2014, 126,3215 –3221;b)T.M.Koh, K. Fu, Y. Fang, S. Chen, T. C. Sum,N.Mathews, S. G. Mhaisalkar,P.P.Boix, T. Baikie, J. Phys. Chem. C 2014, 118,16458–16462.

[41] C. C. Stoumpos, C. D. Malliakas,M.G.Kanatzidis, Inorg.Chem. 2013, 52,9019–9038.

[42] G. E. Eperon, S. D. Stranks, C. Menelaou, M. B. Johnston,L.M.Herz, H. J.Snaith, Energy Environ. Sci. 2014,7,982 –988.

[43] C. K. Møller, Nature 1958, 182,1436 –1436.

[44] D. M. Trots, S. V. Myagkota, J. Phys. Chem.Solids 2008, 69,2520 –2526.

[45] S. Ito, S. Tanaka, K. Manabe, H. Nishino, J. Phys. Chem. C 2014, 118,16995–17000.

[46] T. Leijtens,G.E.Eperon, S. Pathak, A. Abate,M.M.Lee, H. J. Snaith, Nat.Commun. 2013, 4,2885.

[47] N. Aristidou,I.Sanchez-Molina, T. Chotchuangchutchaval,M.Brown, L.Martinez, T. Rath,S.A.Haque, Angew.Chem. Int. Ed. 2015, 54,8208 –8212; Angew.Chem. 2015, 127,8326 – 8330.

[48] a) I. Chung,J.H.Song, J. Im, J. Androulakis, C. D. Malliakas, H. Li, A. J.Freeman, J. T. Kenney,M.G.Kanatzidis, J. Am. Chem. Soc. 2012, 134,8579–8587;b)N.K.Noel, S. D. Stranks, A.

Abate,C.Wehrenfennig, S.Guarnera, A. A. Haghighirad, A. Sadhanala,G.E.Eperon,S.K.Pathak,M. B. Johnston, A. Petrozza, L. M. Herz,H.J.Snaith, Energy Environ. Sci.2014, 7,3061 –3068.

[49] a) T. M. Koh, T. Krishnamoorthy,N.Yantara, C.Shi, W. L. Leong, P. P. Boix,A. C. Grimsdale, S. G. Mhaisalkar,N.Mathews, J. Mater.Chem.A2015, 3,14996–15000; b) S. J. Lee, S. S. Shin, Y. C. Kim,D.Kim, T. K. Ahn,J.H.Noh,J.Seo, S. I. Seok, J. Am. Chem. Soc. 2016, 138,3974 –3977.

[50] V. M. Goldschmidt, Naturwissenschaften 1926, 14,477 –485.

[51] H. S. Kim, S. H. Im, N. G. Park, J. Phys. Chem. C 2014, 118,5615 –5625.

[52] a) C. C. Stoumpos, D. H. Cao, D. J. Clark, J. Young, J. M. Rondinelli, J. I.Jang, J. T. Hupp ,M.G.Kanatzidis, Chem.Mater. 2016, 28,2852 –2867;b) B. V. Beznosikov,K.S.Aleksandrov, Crystallogr.Rep. 2000, 45,792 –798;c)S.N.Ruddlesden,P.Popper, Acta Crystallogr. 1958, 11,54–55;d) R. E. Schaak,T.E.Mallouk,Chem. Mater. 2002, 14,1455 –1471.

[53] S. Gonz#lez-Carrero,R.E.Galian, J. Perez-Prieto, Part. Part. Syst. Charact.2015, 32,709 –720.

[54] Y. Liu, H. Xiao, W. A. Goddard, Nano Lett. 2016, 16,3335 –3340.

[55] K. Chondroudis, D. B. Mitzi, Chem. Mater. 1999, 11,3028 –3030.

[56] M. Yuan, L. N. Quan, R. Comin,G.Walters, R. Sabatini, O. Voznyy,S.Hoogland, Y. Zhao, E. M. Beauregard, P. Kanjanaboos, Z. Lu, D. H. Kim,E. H. Sargent, Nat. Nanotechnol. 2016,inpress,DOI:10.1038/nnano.2016.110.

[57] a) D. Giovanni, W. K. Chong, H. A. Dewi, K. Thirumal, I. Neogi, R. Ramesh,S. Mhaisalkar,N.Mathews,T.C.Sum, Sci. Adv. 2016, 2,e1600477;b) W. K. Chong, K. Thirumal,D.Giovanni,T.W.Goh, X. Liu, N. Mathews,S. Mhaisalkar,T.C.Sum, Phys. Chem. Chem. Phys. 2016, 18,14701–14708.

[58] K. Yao, X. Wang, F. Li, L. Zhou, Chem.Commun. 2015, 51,15430 –15433.

[59] T. M. Koh, V. Shanmugam, J. Schlipf, L. Oesinghaus, P. Meller-Busch-baum, N. Ramakrishnan,V.Swamy,N.Mathews, P. P. Boix, S. G. Mhaisal-kar, Adv.Mater. 2016, 28,3653 –3661.

[60] I. C. Smith, E. T. Hoke, D.Solis-Ibarra, M. D. McGehee, H. I. Karunadasa,Angew.Chem. Int. Ed. 2014, 53,11232–11235; Angew.Chem. 2014, 126,11414 –11417.

[61] D. H. Cao, C. C. Stoumpos, O. K. Farha,J.T.Hupp, M. G. Kanatzidis, J.Am. Chem. Soc. 2015, 137,7843 –7850.

[62] S. Yang, Y. Wang, P. Liu, Y. -B. Cheng, H. J. Zhao, H. G. Yang, Nat. Energy2016, 1,15016.

[63] K. Yao, X. Wang, Y. -x. Xu, F. Li, L. Zhou, Chem. Mater. 2016, 28,3131 –3138.

[64] Y. Hu, J. Schlipf, M. Wussler,M.L.Petrus, W. Jaegermann, T. Bein, P.Meller-Buschbaum, P. Docampo, ACS Nano 2016, 10,5999 –6007.

[65] S. Ahmad, P. K. Kanaujia, H. J. Beeson, A. Abate, F. Deschler, D. Credging-ton, U. SteinerG. V. Prakash,J.J.Baumberg, ACS Appl. Mater. Interfaces2015, 7,25227–25236.ChemSusChem 2016, 9,2541 –2558

[66] C. R. Kagan, D. B. Mitzi, C. D. Dimitrakopoulos, Science 1999, 286,945 –947.

[67] W. Shockley,H.J.Queisser, J. Appl. Phys. 1961, 32,510.

[68] X. Wu, M. T. Trinh, X. Y. Zhu, J. Phys. Chem. C 2015, 119,14714–14721.

[69] K. Tanaka, T. Kondo, Sci. Technol. Adv. Mater. 2003, 4,599 –604.

[70] X. Wu, M. T. Trinh, D. Niesner, H. Zhu, Z. Norman,J.S.Owen, O. Yaffe,B. J. Kudisch, X. Y. Zhu, J. Am. Chem. Soc. 2015, 137,2089 –2096.

[71] a) A. Buin, P. Pietsch, J. Xu, O. Voznyy,A.H.Ip, R. Comin, E. H. Sargent,Nano Lett. 2014, 14,6281 –6286;b)A.Walsh, D. O. Scanlon,S.Chen,X. G. Gong, S.-H. Wei, Angew.Chem. Int. Ed. 2015, 54,1791–1794;Angew.Chem. 2015, 127,1811–1814.

[72] H. Tsai, W. Nie, J.-C. Blancon,C.C.Stoumpos, R. Asadpour, B. Harutyun-yan, A. J. Neukirch, R. Verduzco,J.J.Crochet, S. Tretiak, L. Pedesseau, J.Even, M. A. Alam, G. Gupta, J. Lou, P. M. Ajayan,M.J.Bedzyk,M.G.Ka-natzidis, A. D. Mohite, Nature 2016, 536,312 –316<

[73] a) X. H. Zhu, N. Mercier,A.Riou,P.Blanchard, P. Frere, Chem. Commun.2002,2160–2161;b)D.B.Mitzi, K. Chondroudis, Mo.l Cryst .Liq. Cryst.2001, 356,549–558;c)X.H.Zhu, N. Mercier,P.Frere, P. Blanchard, J.Roncali, M. Allain, C. Pasquier,A.Riou, Inorg.Chem. 2003, 42,5330 –5339.

[74] a) K. Ema, M. Inomata, Y. Kato,H.Kunugita, M. Era, Phys. Rev.Lett. 2008,100,2574 01 ;b)K.Morimoto,K.Matsuishi, J. Phys. Conf. Ser. 2010, 215,012044;c)Y.Y.Li, C. K. Lin, G. L. Zheng, Z. Y. Cheng, H. You, W. D. Wang,J. Lin, Chem. Mater. 2006, 18,3463–3469;d)G.C.Papavassiliou,G.A.Mousdis, G. Pagona, N. Karousis, M. S. Vidali, J. Lumin. 2014, 149,287 –291.

[75] K. Jemli, P. Audebert, L. Galmiche, G. Le Trippe-Allard, D. Garrot, J. S.Lauret, E. Deep orte, ACS Appl. Mater.Interfaces 2015, 7,21763–21769.

[76] A. E. Maughan,J.A.Kurzman, J. R. Neilson, Inorg. Chem. 2015, 54,370 –378.

[77] H. A. Evans, A. J. Lehner,J.G.Labram, D. H. Fabini, O. Barreda, S. R.Smock, G. Wu, M. L. Chabinyc, R. Seshadri, F. Wudl, Chem. Mater. 2016,28,3607 –3611.

[78] X. Li, M. I. Dar,C.Yi, J. Luo, M. Tschumi, S. M. Zakeeruddin, M. K. Nazeer-uddin,H.Han, M. Gr-tzel, Nat. Chem. 2015, 7,703 –711.

[79] D. Bi, P. Gao, R. Scopelliti, E. Oveisi,J.Luo, M. Gr-tzel, A. Hagfeldt, M. K.Nazeeruddin, Adv.Mater. 2016, 28,2910–2915.

[80] Y. Zhao,J.Wei, H. Li, Y. Yan, W. Zhou, D. Yu,Q.Zhao, Nat. Commun.2016, 7,10228.

[81] a) W. Li, W. Zhang, S. VanReenen, R. J. Sutton, J. Fan, A. A. Haghighirad,M. B. Johnston, L. Wang, H. J. Snaith, Energy Environ. Sci. 2016, 9,490 –498;b)I.Hwang, M. Baek,K.Yong, ACS Appl.Mater. Interfaces 2015, 7,27863–27870.

[82] a) S. Guarnera, A. Abate, W. Zhang, J. M. Foster,G.Richardson, A. Petroz-za, H. J. Snaith, J. Phys. Chem. Lett. 2015, 6,432 –437;b)X.Dong, X.Fang, M. Lv,B.Lin, S. Zhang, J. Ding, N. Yuan, J. Mater. Chem. A 2015, 3,5360–5367;c)G.Niu, W. Li, F. Meng, L. Wang, H. Dong, Y. Qiu, J. Mater.Chem. A 2014, 2,705 –710.

[83] J. Song,E.Zheng, J. Bian, X.-F.Wang, W. Tian, Y. Sanehira, T. Miyasaka, J.Mater.Chem.A2015, 3,10837 –10844.

[84] J. Song,J.Bian, E. Zheng, X.-F.Wang, W. Tian, T. Miyasaka, Chem.Lett.2015, 44,610 –612.

[85] a) J. H. Kim, P. -W.Liang, S. T. Williams, N. Cho, C.-C. Chueh, M. S. Glaz,D. S. Ginger,A.K.Y.Jen, Adv. Mater. 2015, 27,695–701;b)J.You, L.Meng, T.-B. Song, T.-F.Guo, Y. Yang, W.-H. Chang, Z. Hong, H. Chen, H.Zhou, Q. Chen,Y.Liu, N. De Marco,Y.Yang, Nat. Nanotechnol. 2016, 11,75–81.

[86] W. Chen,Y.Wu, Y. Yue, J. Liu, W. Zhang, X. Yang, H. Chen, E. Bi, I. Ashra-ful, M. Gr-tzel, L. Han, Science 2015, 350,944 –948.

[87] a) D. Bi, G. Boschloo, A. Hagfeldt, Nano 2014, 9,1440001;b)S.Aharon,S. Gamliel, B. El Cohen, L. Etgar, Phys. Chem. Chem. Phys. 2014, 16 ,10512–10518.

[88] A. Mei, X. Li,L.Liu, Z. Ku,T.Liu, Y. Rong, M. Xu, M. Hu, J. Chen,Y.Yang,M. Gr-tzel, H. Han, Science 2014, 345,295 –298.

[89] a) J. Chen,Y.Rong, A. Mei, Y. Xiong, T. Liu, Y. Sheng, P. Jiang, L. Hong, Y.Guan, X. Zhu,X.Hou,M.Duan, J. Zhao, X. Li, H. Han, Adv.EnergyMater.2016, 6,1502009;b)Z.Wei, H. Chen, K. Yan, S. Yang, Angew.Chem.Int.Ed. 2014, 53,13239 –13243; Angew.Chem. 2014, 126,13455 –13459;c) Z. Wei, X. Zheng, H. Chen,X.Long, Z. Wang,S.Yang, J. Mater.Chem.A 2015, 3,16430–16434;d)F.Zhang, X. Yang, H. Wang, M. Cheng, J.Zhao, L. Sun, ACS Appl. Mater.Interfaces 2014, 6 ,16140 –16146;e)C.-Y.Chan, Y. Wang, G.-W.Wu, E. W.-G. Diau, J. Mater.Chem. A 2016, 4,3872 –3878;f)H.Li, K. Cao, J. Cui, S. Liu, X. Qiao, Y. Shen, M. Wang, Nanoscale2016, 8,6379 –6385.

[90] M. Kaltenbrunner,G.Adam,E.D.Glowacki, M. Drack, R. Schwoediauer,L. Leonat, D. H. Apaydin, H. Groiss, M. C. Scharber,M.S.White, N. S. Sari-ciftci, S. Bauer, Nat. Mater. 2015, 14,1032 –1039.

[91] I. Hwang, I. Jeong, J. Lee, M. J. Ko, K. Yong, ACS Appl. Mater.Interfaces2015, 7,17330–17336.[92] H. C. Weerasinghe, Y. Dkhissi, A. D. Scully,R.A.Caruso,Y.-B. Cheng,NanoEnergy 2015, 18,118–125.